Line and Lattice Networks under Deterministic Interference Models

Jasper Goseling, Michael Gastpar and Jos H. Weber

Abstract

Capacity bounds are compared for four different deterministic models of wireless networks, representing four different ways of handling broadcast and superposition in the physical layer. In particular, the transport capacity under a multiple unicast traffic pattern is studied for a one-dimensional network of regularly spaced nodes on a line and for a two-dimensional network of nodes placed on a hexagonal lattice. The considered deterministic models are: (i) P/P, a model with exclusive transmission and reception, (ii) P/M, a model with simultaneous reception of the sum of the signals transmitted by all nearby nodes, (iii) B/P, a model with simultaneous transmission to all nearby nodes but exclusive reception, and (iv) B/M, a model with both simultaneous transmission and simultaneous reception. All four deterministic models are considered under half-duplex constraints. For the one-dimensional scenario, it is found that the transport capacity under B/M is twice that under P/P. For the two-dimensional scenario, it is found that the transport capacity under B/M is at least 2.5 times, and no more than six times, the transport capacity under P/P. The transport capacities under P/M and B/P fall between these bounds.

Index Terms

Capacity, Network Coding, Deterministic Model, Multi-source, Multi-commodity, Computation Codes

I. Introduction

The promise of network coding is the subject of an extensive and growing body of literature, starting with [1] and leading to several textbooks, a few recent examples being [2]–[4]. The basic insight provided in [1] is that intermediate nodes in a network need not always forward all the information they receive. Rather, it can be sufficient for them to forward merely a function of that information.

A natural follow-up observation is that if intermediate nodes are merely forwarding a function of their received information, then they actually do not have to receive all that information in the first place. Rather, as long as they manage to receive the particular function they need to forward, the overall networking solution will work properly. This is where *interference* enters the picture. As was shown in [5], [6], whenever signals interfere, it can

J. Goseling, M. Gastpar and J.H. Weber are with Faculty of EEMCS, Delft University of Technology, Mekelweg 4, 2628 CD Delft, The Netherlands. (email: j.goseling@ieee.org, gastpar@eecs.berkeley.edu, j.h.weber@tudelft.nl) J. Goseling is also with Department of Applied Mathematics, University of Twente, Drienerlolaan 5, 7522 NB Enschede, The Netherlands. M. Gastpar is also with Department of Electrical Engineering and Computer Sciences, University of California, Berkeley, CA 94720-1770.

be more efficient for the decoder to obtain only a function of the transmitted messages, rather than all the messages individually. This is particularly interesting for the wireless medium where interference is linear. More precisely, in wireless networks, two physical effects are waiting to be exploited:

Broadcast: The first aspect of the phenomenon of interference is that any transmitted signal not only impacts the desired receiver, but all receivers within a certain spatial range. The obvious positive aspect of this is that with the same resource investment (time, spectrum, energy), multiple receivers could be served simultaneously. In a network context this can be very beneficial and it has been the topic of numerous studies. Some of the directions that have been investigated are exploiting the broadcast in combination with network coding to increase throughput [7], [8], reduce energy consumption [9]–[11], or reduce queue backlogs [12].

Superposition: The second aspect is that if multiple nodes transmit simultaneously, then a receiving node that is within range of all of those transmitters receives a linear superposition of the transmitted signals. A classical way of treating this is to consider any superposition an erasure/collision and to use clever scheduling to avoid this effect from occurring. However, more sophisticated approaches to physical-layer coding can deal with such linear superposition in other ways. For one, a receiver can first decode one signal, treating all others as noise. Then, assuming the decoding was correct, that signal can be subtracted from the received signal. This is referred to as successive cancellation decoding. In this paper, we will not consider this option. Instead, we will consider a new way of exploiting the same superposition effect: Namely, to decode a *function* of the transmitted messages at a high rate. In particular, the function that is decoded is the *sum* of the messages. The idea of exploiting superposition in this way has been the topic of [5], [6] as well as many other recent studies, some of which will be reviewed in Section II.

The classical means of operating a wireless network, turning the physical layer into a network of reliable point-to-point bit pipes, removes both broadcast and superposition. This results in an abstraction of the wireless medium in which reliable communication is most naturally captured by a deterministic model. In this paper we introduce other deterministic models, capturing the effects of exploiting broadcast and/or superposition by decoding linear functions. We study four models that are denoted as P/P, B/P, P/M and B/M. The first position denotes whether symbols are transmitted to a single neighbour (P(oint-to-point)) or to all neighbours (B(roadcast)). The second position denotes whether multiple transmissions to a node cause interference (P(oint-to-point)) or that nodes receive the sum of all symbols that are transmitted by neighbours (M(ulti-acces)). More precisely we introduce the following models:

1) P/P: Neither broadcast nor superposition are exploited, *i.e.*, a single transmission can be received by at most one device and multiple transmissions to the same device result in a collision.
2) B/P: Transmissions are received by all neighbours. However, multiple transmissions to the same device lead to a collision.
3) P/M: Nodes can decode the sum of all transmissions by neighbouring nodes. However, a single transmission can be received by at most one device.
4) B/M: Finally, the most interesting deterministic network model considered in this paper is the combination of the above two effects into a model that involves both the broadcast and the superposition effects.

Our goal in this paper is to compare the performance attainable under these four deterministic models. For the performance measure in this paper, we study achievable rates for *multiple unicast connections,* i.e., messages of every source node are of interest only to one destination node. This is by contrast to several other problems of interest, such as for example the multi-casting problem where one source node may be of interest to many destinations. Finally, the particular figure of merit that we consider in this paper will be the so-called *transport capacity:* For each source-destination pair, we evaluate the product of the rate achieved and the distance between source and destination. The transport capacity of the network, as introduced in [13], is then the sum of all of these products, maximized over all possible placements of unicast connections. Obviously, there are other interesting performance measures to study, for instance, the maximum achievable common rate in a random multiple unicast configuration, as studied in many recent papers like, for instance [14], [15]. Since no single number can fully characterize 'the' capacity of a network we believe that several performance measures should be explored.

We establish upper and lower bounds on the transport capacity under the four different deterministic network models for two specific arrangements of the nodes in the network. Our results are the following:

1) We consider a network where all the nodes are arranged in a line and obtain tight capacity bounds for all models. We find that the capacity under $\mathsf{B/P}$ and $\mathsf{P/M}$ is 33% larger than the capacity under $\mathsf{P/P}$. Moreover, the capacity under $\mathsf{B/M}$ is twice the capacity under $\mathsf{P/P}$.
2) We consider a network where the nodes are arranged on a two-dimensional hexagonal lattice. Here we find that the capacity under $\mathsf{B/M}$ is at least 2.5 times, and no more than six times, the transport capacity under $\mathsf{P/P}$. The transport capacities under $\mathsf{P/M}$ and $\mathsf{B/P}$ fall between these bounds.

For the line network our upper and lower bounds are tight in the sense that the difference is a constant independent of the network size. For the two-dimensional case our bounds are not tight. Finding the optimal network coding solution for multiple unicast appears to be a hard (and open) problem. This claim is supported by the fact that linear network codes are not sufficient to achieve capacity [16].

By contrast to a growing body of literature on deterministic models, see *e.g.*, [17]–[21], our main emphasis is not on (approximate) capacity results. Instead, we consider maximum attainable performance under specific operating constraints. For the $\mathsf{P/P}$ model these operating constraints correspond to first reducing the wireless medium to a network of reliable point-to-point links. For the other models considered in this paper there is also a reduction to reliable links, but these are no longer point-to-point. All models correspond, in a sense, to different means of handling the wireless medium in a (OSI) layered overall system architecture. Indeed, we will see in this paper how our results can be applied to obtain achievable rates for Gaussian network models by specifically considering a simple version with local interference only.

The paper is organized as follows. In Section II we review some of the recent work on exploiting superposition. In Section III, we introduce the problem and the four different deterministic interference models that are considered. In Section IV we provide upper and lower bounds. In Sections V and VI we present proofs of our bounds. In Section VII we outline the application of our results to Gaussian network models. In Section VIII we conclude this paper with a discussion of the results.

II. Computation Coding

Exploiting superposition in combination with network coding by recovering a sum of different messages has been considered in many recent papers. The concept is known under various names, such as analog network coding [22], [23], physical layer network coding [24]–[28], joint physical layer coding and network coding [29], [30], layer-2 combining [31] and computation coding [5], [6], [32], [33].

Many of the recent studies [22], [24]–[26], [28], [31] have focussed on uncoded transmissions and the corresponding detection problems. In these works the performance of these strategies in communicating a single sum of messages to a specific receiver is analyzed. In [22] the influence of imperfect synchronization between nodes is considered and measurement results from a testbed are presented. The diversity-multiplexing tradeoff of a physical-layer network coding system is studied in [28]. Of course, if these uncoded strategies are used in larger networks a method will need to be devised to prevent the amplification of noise and/or the propagation of errors. This problem has not been adressed in previous work based on uncoded transmissions. In [24] the benefit of physical layer network coding in a line network is studied under the assumption that there is no propagation of errors.

By contrast to performing uncoded transmissions, our focus is reliable communication over each link. In [6] it has been demonstrated that if N nodes communicate to a single receiver in a Gaussian multiple-access channel, the maximum achievable rate R for reliable communication satisfies

$$\frac{1}{2}\log\left(\frac{1}{N}+P\right) \leq R \leq \frac{1}{2}\log(1+P), \tag{1}$$

where P is an individual power constraint for each of the transmitters. Starting from the results in [6] we assume that nodes are able to reliably decode the sum of the messages. Similar arguments have been used for specific small network examples, e.g., [29], [30], [32], [33]. The difference with our work is that we consider networks of arbitrary size.

In [27] the scaling behaviour of the capacity of random networks is studied under physical-layer network coding. It is shown that exploiting superposition by decoding sums of messages does not affect the scaling behaviour. Our focus is on networks with specific node placement and analysis of the constants involved.

III. Model and Notation

A. Network

We model a wireless network as a directed graph (V, E), where V is the set of nodes and $E \subseteq V \times V$ are the edges. If $(u, v) \in E$, information can be reliably transmitted from u to v. The interaction between nodes is specified in more detail below for each of the four models. We assume that $(u, v) \in E$ implies $(v, u) \in E$, *i.e.*, that the interaction between nodes is symmetric.

B. Communication Models

Time is slotted. Symbols are from the finite field $\mathbb{F}_q$. In the remainder the base of the logarithm in entropy and mutual information measures is q, *i.e.*, the unit of information is the q-ary symbol. In all four models each link can carry one q-ary symbol per time slot. Hence the links have unit capacity. Let $X_v[t]$ and $Y_v[t]$ be the symbols transmitted and received respectively, by node v in time slot t. For $S \subseteq V$, let $X^S[t] = \{X_v[t] | v \in S\}$ and $Y^S[t] = \{Y_v[t] | v \in S\}$. Let

$$N_v = \{w \in V | (v, w) \in E\} \cup \{v\}, \tag{2}$$

i.e., N_v is the neighbourhood of v including v itself. The channel output Y_v depends only on X^{N_v}, the channel inputs of neighbouring nodes in the same time slot. The relation between Y_v and X^{N_v} is independent of time and therefore dependence on the time slot is often omitted in the notation.

All our models will respect half-duplex constraints, meaning that no node can simultaneously transmit and receive. Formally, we model this by extending the channel input alphabet with a "silent" symbol σ denoting that a node is not transmitting. Moreover, formally, for any node v that is transmitting in time slot t, its corresponding received signal $Y_v[t]$ is set to an independent random variable, uniformly distributed over the entire alphabet. This means that v does not get any information.[1] We restrict our attention to transmission strategies in which the transmission schedule is fixed ahead of time, *i.e.*, strategies for which

$$P(X_v[t] = \sigma) \in \{0, 1\}. \tag{3}$$

Note that even though half-duplex constraints are modelled by means of a uniformly distributed channel output, the model is otherwise deterministic in nature.

The exact functional relation is now specified for each of the models that were introduced in Section I. The four models are denoted by P/P, B/P, P/M and B/M. The first position denotes whether symbols are transmitted to a single neighbour (P) or broadcast to all neighbours (B). The second position denotes whether multiple transmissions to a node cause interference (P) or that nodes receive the sum of all symbols that are transmitted by neighbours (M). To simplify notation we introduce random variables Z_v, $v \in V$, uniformly distributed over $\mathbb{F}_q$. Each Z_v is independent of all other random variables. In addition, for the P/P and P/M models we introduce, for each node $v \in V$, a variable A_v that denotes the neighbour that v is transmitting to. Since the transmission schedule is fixed ahead of time

$$P(A_v[t] = w) \in \{0, 1\}, \tag{4}$$

for all $v, w \in V$.

The models are defined as follows.

P/P: Neither broadcast nor superposition are exploited, *i.e.*, a single transmission can be received by at most one device and multiple transmissions to the same device result in a collision. This means that $Y_v = X_u$ if u is the only neighbour of v that is transmitting and also v itself is not transmitting. Otherwise $Y_v = Z_v$, *i.e.*, a uniformly

[1]Another way to model collisions due to interference, would be to extend the output alphabet with an erasure symbol. This, however, creates a covert channel.

distributed random variable. This gives

$$\mathsf{P/P}: \quad Y_v = \begin{cases} X_u, & \text{if } u \in N_v, X_u \neq \sigma, A_u = v, \forall w \in N_v \setminus \{u\}\colon X_w = \sigma, \\ Z_v, & \text{otherwise.} \end{cases} \tag{5}$$

P/M: Superposition is exploited, but broadcast is not. A transmission from u to v prevents other transmissions from u, but other transmissions to v are allowed. If v is not transmitting itself, it receives the sum of all symbols that are transmitted to v by its neighbours, *i.e.*,

$$\mathsf{P/M}: \quad Y_v = \begin{cases} \sum_{u \in N_v : X_u \neq \sigma} X_u, & \text{if } X_v = \sigma \text{ and } \exists u \in N_v\colon X_u \neq \sigma \text{ and } \forall w \in N_v\colon (X_w \neq \sigma \rightarrow A_w = v), \\ Z_v, & \text{otherwise.} \end{cases} \tag{6}$$

B/P: Broadcast is exploited, but superposition is not. A transmission from u to v prevents other transmissions to v, but other transmissions from u are allowed. Since u is broadcasting to all its neighbours we don't need the variables A_v in the B/P model. This gives

$$\mathsf{B/P}: \quad Y_v = \begin{cases} X_u, & \text{if } u \in N_v, X_u \neq \sigma, \forall w \in N_v \setminus \{u\}\colon X_w = \sigma, \\ Z_v, & \text{otherwise.} \end{cases} \tag{7}$$

B/M: Both broadcast and superposition are exploited. Each node that is not transmitting receives the sum of the symbols transmitted by all its neighbours, *i.e.*,

$$\mathsf{B/M}: \quad Y_v = \begin{cases} \sum_{u \in N_v : X_u \neq \sigma} X_u, & \text{if } X_v = \sigma \text{ and } \exists u \in N_v : X_u \neq \sigma, \\ Z_v, & \text{otherwise.} \end{cases} \tag{8}$$

C. Transport Capacity

The traffic pattern that we consider is multiple unicast. For a set of K unicast sessions, let S_k and D_k denote the source and destination respectively, of the kth session, and R_k its throughput. Each subset $\Gamma \subseteq V$ of nodes induces a partition of V and hence a directed cut. We will, therefore, often refer to a set of nodes as a cut. For $\Gamma \subseteq V$, let $\bar{\Gamma} = V \setminus \Gamma$ and

$$K_\Gamma = \{k | S_k \in \Gamma, D_k \notin \Gamma\}. \tag{9}$$

Our measure of interest is the *transport capacity* of a network which is defined as the maximum, over all configurations of unicast sessions on a given network and all possible transmission strategies, of $\sum_{k=1}^{K} \operatorname{dist}(S_k, D_k) R_k$, where $\operatorname{dist}(S_k, D_k)$ is the number of hops on the shortest path from S_k to D_k, *i.e.*, the transport capacity is the maximum number of q-ary symbols $\times$ hops per time slot that can be transported in the network. We will derive upper and lower bounds on the transport capacity of some networks under the different models.

D. Notation

Finally, we define some notation. If $f(L) = \mathrm{o}(g(L))$ for a function $f : \mathbb{N} \to \mathbb{R}$ then

$$\lim_{L\to\infty} \frac{f(L)}{g(L)} = 0.$$

Similarly, $f(L, M) = \mathrm{o}(g(L, M))$ for a function $g : \mathbb{N}^2 \to \mathbb{R}$ means that

$$\lim_{L\to\infty} \frac{f(L, L)}{g(L, L)} = 0.$$

The floor and ceiling operations are denoted by $\lfloor x \rfloor$ and $\lceil x \rceil$ respectively, *i.e.*, $\lfloor x \rfloor = \max\{y \in \mathbb{Z} \mid y \leq x\}$ and $\lceil x \rceil = \min\{y \in \mathbb{Z} \mid y \geq x\}$. For integers a, b and $p > 0$, $a \equiv b \pmod{p}$ means that a and b are congruent modulo p, *i.e.*, that $a - b$ is divisible by p. Finally, $a = b \pmod{p}$ means that the remainder of a divided by p is b.

IV. Main Results

A. Line Network

We consider the line network represented by (V, E), where

$$V = \{0, 1, \ldots, L\}, \quad E = \{(u, v) \subseteq V \times V \mid |u - v| = 1\}. \tag{10}$$

The throughput of multiple unicast on the line network in a model that allows for broadcast and coding was first studied in [7]. The extension to models that allow for superposition has been treated in [22], [24]. We give bounds on the transport capacity of the line network under the different models. The coding scheme used to achieve the lower bounds was also used in previous work [7], [22], [24]. Results similar to Theorems 2 and 4 have appeared in [7] and [24] respectively. The proof techniques that are developed are new and will be used to analyze the hexagonal lattice. For the P/P and B/M models we have exact results for the transport capacity of the line network. For the B/P and P/M models we provide upper and lower bounds that are separated by at most $\frac{2}{3}$.

Theorem 1. *The transport capacity $C^{\mathrm{line}}_{\mathsf{P/P}}(L)$ of the $L + 1$ node line network under the* P/P *model is*

$$C^{\mathrm{line}}_{\mathsf{P/P}}(L) = \left\lceil \frac{1}{2} L \right\rceil.$$

Theorem 2. *The transport capacity $C^{\mathrm{line}}_{\mathsf{B/P}}(L)$ of the $L + 1$ node line network under the* B/P *model satisfies*

$$\frac{2}{3} L \leq C^{\mathrm{line}}_{\mathsf{B/P}}(L) \leq \left\lceil \frac{2}{3} L \right\rceil.$$

Theorem 3. *The transport capacity $C^{\mathrm{line}}_{\mathsf{P/M}}(L)$ of the $L + 1$ node line network under the* P/M *model satisfies*

$$\frac{2}{3} L \leq C^{\mathrm{line}}_{\mathsf{P/M}}(L) \leq \left\lceil \frac{2}{3} L \right\rceil.$$

Theorem 4. *The transport capacity $C^{\mathrm{line}}_{\mathsf{B/M}}(L)$ of the $L + 1$ node line network under the* B/M *model is*

$$C^{\mathrm{line}}_{\mathsf{B/M}}(L) = L.$$

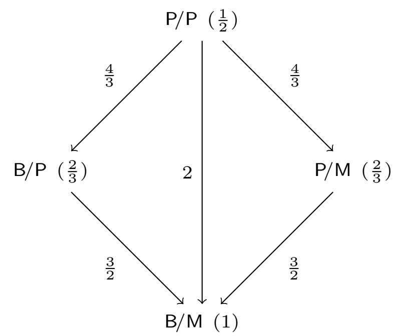

Fig. 1. Transport capacity of the line network under different models. For each model in parentheses is $\lim_{L\to\infty} \frac{C^{\text{line}}(L)}{L}$. Labels next to arrows denote the multiplicative improvement obtained by moving from one model to the next.

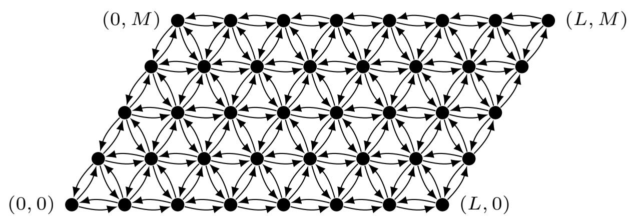

Fig. 2. Nodes located at the hexagonal lattice with connectivity between nearest neighbours, $L = 7$, $M = 4$.

Fig. 1 gives an overview of the results from Theorems 1–4. The figure presents the value of $\lim_{L\to\infty} \frac{C^{\text{line}}(L)}{L}$ for each model. Moreover, the labels next to arrows denote the multiplicative improvement obtained by moving from one model to the next. One can observe that moving from P/P to B/P or P/M gives an improvement of approximately 33%. However, the combined effect of B/P and P/M, *i.e.*, moving from P/P to B/M gives an improvement of 100%. Note that the combined effects of multiaccess and broadcast are larger than the sum of their individual contributions. We will provide some intuition for this in Section V-A.

B. Hexagonal Network

In this section we consider a network of size $(L+1)\times(M+1)$ with nodes located on the hexagonal lattice and edges between nearest neighbours. We index nodes with a tuple $(u_1, u_2) \in \mathbb{N}^2$. The location in $\mathbb{R}^2$ of (u_1, u_2) is $(u_1, u_2)G_\Lambda$, with $G_\Lambda = \begin{bmatrix} 1 & 0 \\ 1/2 & \sqrt{3}/2 \end{bmatrix}$. Now, we consider (V, E) with

$$V = \{(u_1, u_2) \mid \ 0 \le u_1 \le L, 0 \le u_2 \le M\},$$

$$E = \{((u_1, u_2), (v_1, v_2)) \subset V \times V \mid \ \|(u_1 - v_1, u_2 - v_2)G_\Lambda\|_2 = 1\}.$$

The hexagonal network is illustrated in Figure 2. Note, that the number of edges in (V, E) is $6LM + 2(L + M)$.

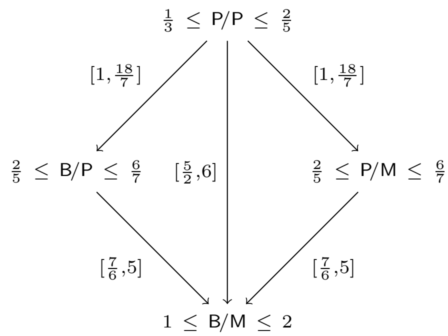

Fig. 3. Transport capacity of the hexagonal lattice under different models, assuming $q = 2$. For each model lower and upper bounds on $\lim_{L\to\infty,M\to\infty} \frac{C^{\text{hex}}(L,M)}{LM}$ are presented. Labels next to arrows denote the range (lower and upper bounds) of the multiplicative improvement obtained by moving from one model to the next.

Theorem 5. *The transport capacity $C^{\text{hex}}_{\mathsf{P/P}}(L,M)$ of the $(L+1)\times(M+1)$ node hexagonal network under the* P/P *model satisfies*

$$\frac{1}{3}LM + \mathrm{o}(LM) \le C^{\text{hex}}_{\mathsf{P/P}}(L,M) \le \frac{2}{5}LM + \mathrm{o}(LM).$$

Theorem 6. *The transport capacity $C^{\text{hex}}_{\mathsf{P/M}}(L,M)$ of the $(L+1)\times(M+1)$ node hexagonal network under the* P/M *model satisfies*

$$\frac{2}{5}LM + \mathrm{o}(LM) \le C^{\text{hex}}_{\mathsf{P/M}}(L,M) \le \frac{6}{7}LM + \mathrm{o}(LM).$$

Theorem 7. *The transport capacity $C^{\text{hex}}_{\mathsf{B/P}}(L,M)$ of the $(L+1)\times(M+1)$ node hexagonal network under the* B/P *model satisfies*

$$\frac{2}{5}LM + \mathrm{o}(LM) \le C^{\text{hex}}_{\mathsf{B/P}}(L,M) \le \frac{6}{7}LM + \mathrm{o}(LM).$$

Theorem 8. *The transport capacity $C^{\text{hex}}_{\mathsf{B/M}}(L,M)$ of the $(L+1)\times(M+1)$ node hexagonal network under the* B/M *model satisfies*

$$C^{\text{hex}}_{\mathsf{B/M}}(L,M) \le 2LM + \mathrm{o}(LM).$$

Moreover, if $q = 2$, then it satisfies

$$C^{\text{hex}}_{\mathsf{B/M}}(L,M) \ge LM + \mathrm{o}(LM).$$

Note that the lower bound of the above theorem holds only for $q = 2$. We do not believe that $q = 2$ is a necessary condition, but have not been able to prove the result for arbitrary q. Based on the proof techniques used for Theorems 6 and 7 it is possible to obtain other (weaker) lower bounds for arbitrary q, but for the purpose of clarity of exposition those have been omitted from this paper.

Fig. 3 gives an overview of the results from Theorems 5–8. The figure presents lower and upper bounds to the value of $\lim_{L\to\infty,M\to\infty} \frac{C^{\text{hex}}(L,M)}{LM}$ for each model. Moreover, the labels next to arrows denote the range (upper and lower bounds) of the multiplicative improvement obtained by moving from one model to the next.

V. Upper Bounds

In this section we give proofs for the upper bounds of Theorems 1–8. In Subsection V-A constraint graphs are introduced that capture the structure of the topology and some of the constraints imposed by the communication models. Subsection V-B deals with upper bounds for the line network. The upper bounds for the hexagonal lattice are derived in Subsection V-C.

A. Constraint graphs

We capture some of the structure of the topology and the communication models in (undirected) graphs $(E, \mathcal{J}_{\mathsf{B/M}})$, $(E, \mathcal{J}_{\mathsf{B/P}})$, $(E, \mathcal{J}_{\mathsf{P/M}})$ and $(E, \mathcal{J}_{\mathsf{P/P}})$. These graphs capture the idea that if $\langle (u,v),(u',v')\rangle$ is an edge, then it is not possible that $I(X_u;Y_v)$ and $I(X_{u'};Y_{v'})$ are both positive. Before specifying the constraint graphs precisely, we provide some intuition. We consider Fig. 4, depicting subsets of edges of the line network, and first focus on the $\mathsf{P/P}$ model, Fig. 4(a). Assume that $I(X_2;Y_3) > 0$, *i.e.*, that information is transmitted across the thick edge $(2,3)$ in the network. Then, for all other edges (u',v') in the figure it is true that under the $\mathsf{P/P}$ model $I(X_{u'};Y_{v'}) = 0$. We discuss why this is true for each of these edges. First, remember that one of the assumptions made in Section III is that the transmission schedule is fixed ahead of time, *i.e.*, that for all $v \in V$, $P(X_v = \sigma) \in \{0,1\}$ and $P(A_v = u) \in \{0,1\}$. Together with (5) this implies that $I(X_2;Y_3) > 0$ gives

$$P(X_2 = \sigma) = 0, \quad P(X_3 = \sigma) = 1, \quad P(A_2 = 3) = 1. \tag{11}$$

Now, again from (5), achieving $I(X_1;Y_2) > 0$ or $I(X_3;Y_2) > 0$ on edges $(1,2)$ or $(3,2)$ respectively, would require $X_2 = \sigma$, contradicting (11). In other words transmissions to node 2 are not possible due to half-duplex constraints. In similar fashion $I(X_3;Y_4) > 0$ would violate half-duplex constraints, since it requires $X_3 \neq \sigma$. Achieving $I(X_2;Y_1) > 0$ would require $A_2 = 1$, which again contradicts (11). Note that under the $\mathsf{B/P}$ and $\mathsf{B/M}$ models, *i.e.*, when broadcast can be exploited, $I(X_2;Y_1)$ and $(X_2;Y_3)$ can be simultaneously positive. Achieving $I(X_4;Y_3) > 0$ would require $X_4 \neq \sigma$. However, by (5), it is not possible to have node $4 \in N_3 \setminus \{2\}$ to transmit. In other words: a transmission from node 4 causes a collision at 3. Under the $\mathsf{P/M}$ and $\mathsf{B/M}$ models, *i.e.*, when superposition is exploited, $I(X_4;Y_3)$ and $(X_2;Y_3)$ can be simultaneously positive. Finally, similar arguments hold for edges $(0,1)$ and $(4,5)$. It can be seen that $I(X_0;Y_1)$ and $I(X_4;Y_5)$ can only be positive under the $\mathsf{B/M}$ model, *i.e.*, if both broadcast and interference are exploited. In the next four lemmas we define the constraints graphs for arbitrary networks and for all four models. An extension to the above ideas is that we allow for arbitrary conditioning in the mutual information terms. Note that we do not allow for loops in the constraint graphs, *i.e.*, $\langle (u,v),(u,v)\rangle$ is never an edge.

Lemma 1. *Consider the* $\mathsf{P/P}$ *model and let* $\mathcal{J}_{\mathsf{P/P}}$*, a set of unorderded pairs of* E*, be defined as*

$$\Big\langle (u,v),(u',v')\Big\rangle \in \mathcal{J}_{\mathsf{P/P}} \text{ iff } u' \in N_v \text{ or } u \in N_{v'}. \tag{12}$$

Consider arbitrary subsets $U, W, U', W' \subseteq V$ *and assume* $\langle (u,v),(u',v')\rangle \in \mathcal{J}_{\mathsf{P/P}}$*. There does not exist a joint distribution on* X^V *and* A^V *satisfying* $P(X_w = \sigma) \in \{0,1\}$ *and* $P(A_w = w') \in \{0,1\}$ *for all* $w, w' \in V$ *such* *that both* $I(X_u, A_u; Y_v | X^U, A^U, Y^W) > 0$ *and* $I(X_{u'}, A_{u'}; Y_{v'} | X^{U'}, A^{U'}, Y^{W'}) > 0$.

Proof: Assume $I(X_u, A_u; Y_v | X^U, A^U, Y^W) > 0$ and $I(X_{u'}, A_{u'}; Y_{v'} | X^{U'}, A^{U'}, Y^{W'}) > 0$. By (3), (4) and (5) we have

$$P(X_u = \sigma) = 0, \tag{13}$$

$$P(A_u = v) = 1, \tag{14}$$

$$P(X_w = \sigma) = 1, \text{ for all } w \in N_v \setminus \{u\}, \tag{15}$$

$$P(X_{u'} = \sigma) = 0, \tag{16}$$

$$P(A_{u'} = v') = 1, \text{ and} \tag{17}$$

$$P(X_{w'} = \sigma) = 1, \text{ for all } w' \in N_{v'} \setminus \{u'\}. \tag{18}$$

Since $\langle (u, v), (u', v') \rangle \in \mathcal{J}_{\mathsf{P/P}}$, we have $u' \in N_v$ or $u \in N_{v'}$. Now, if $u \neq u'$, then $u' \in N_v \setminus \{u\}$ or $u \in N_{v'} \setminus \{u'\}$ and we have a contradiction between (15) and (16) or (13) and (18) respectively. If $u = u'$ then $v' \neq v$, since $(u, v) \neq (u', v')$ and we obtain a contradiction between (14) and (17). ■

Lemma 2. *Consider the* P/M *model and let* $\mathcal{J}_{\mathsf{P/M}}$*, a set of unorderded pairs of* E*, be defined as*

$$\Big\langle (u, v), (u', v') \Big\rangle \in \mathcal{J}_{\mathsf{P/M}} \textit{ iff } v' \neq v \textit{ and } (u' \in N_v \textit{ or } u \in N_{v'}). \tag{19}$$

Consider arbitrary subsets $U, W, U', W' \subseteq V$ *and assume* $\Big\langle (u, v), (u', v') \Big\rangle \in \mathcal{J}_{\mathsf{P/M}}$. *There does not exist a joint distribution on* X^V *and* A^V *satisfying* $P(X_w = \sigma) \in \{0, 1\}$ *and* $P(A_w = w') \in \{0, 1\}$ *for all* $w, w' \in V$ *such that both* $I(X_u, A_u; Y_v | X^U, A^U, Y^W) > 0$ *and* $I(X_{u'}, A_{u'}; Y_{v'} | X^{U'}, A^{U'}, Y^{W'}) > 0$.

Proof: Assume $I(X_u, A_u; Y_v | X^U, A^U, Y^W) > 0$ and $I(X_{u'}, A_{u'}; Y_{v'} | X^{U'}, A^{U'}, Y^{W'}) > 0$. By (3), (4) and (6) we have

$$P(X_u = \sigma) = 0, \tag{20}$$

$$P(A_u = v) = 1, \tag{21}$$

$$P(X_w = \sigma) = 0 \longrightarrow P(A_w = v) = 1, \text{ for all } w \in N_v, \tag{22}$$

$$P(X_{u'} = \sigma) = 0, \tag{23}$$

$$P(A_{u'} = v') = 1, \text{ and} \tag{24}$$

$$P(X_{w'} = \sigma) = 0 \longrightarrow P(A_{w'} = v') = 1, \text{ for all } w' \in N_{v'}. \tag{25}$$

Suppose that $u' \in N_v$. By (22) and (23) we need $P(A_{u'} = v) = 1$, but this contradicts (24), since $v' \neq v$. In similar fashion (20), (21) and (25) contradict in the case that $u \in N_{v'}$. ■

Lemma 3. *Consider the* B/P *model and let* $\mathcal{J}_{\mathsf{B/P}}$*, a set of unorderded pairs of* E*, be defined as*

$$\Big\langle (u, v), (u', v') \Big\rangle \in \mathcal{J}_{\mathsf{B/P}} \quad \textit{iff} \quad u' \in N_v \setminus \{u\} \textit{ or } u \in N_{v'} \setminus \{u'\}. \tag{26}$$

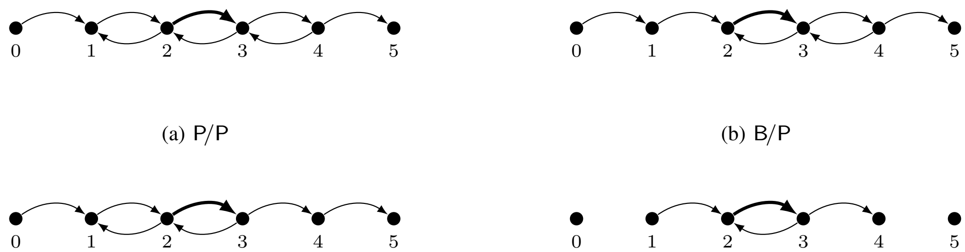

(a) P/P (b) B/P

(c) P/M (d) B/M

Fig. 4. Illustration of the constraint graphs of the line network under the various models. In thin lines the edges that interfere with the thick edge, *i.e.*, in thin lines the set of edges (u', v') for which $\langle (u,v),(u',v') \rangle$ is in the constraint graph, where (u,v) is the thick edge.

Consider arbitrary subsets $U, W, U', W' \subseteq V$ *and assume* $\langle (u,v),(u',v') \rangle \in \mathcal{J}_{\mathsf{B/P}}$*. There does not exist a joint distribution on* X^V *satisfying* $P(X_w = \sigma) \in \{0,1\}$ *for all* $w \in V$ *such that both* $I(X_u; Y_v | X^U, Y^W) > 0$ *and* $I(X_{u'}; Y_{v'} | X^{U'}, Y^{W'}) > 0$.

Proof: Assume $I(X_u; Y_v | X^U, Y^W) > 0$ and $I(X_{u'}; Y_{v'} | X^{U'}, Y^{W'}) > 0$. By (3) and (7) we have $P(X_u = \sigma) = 0$, $P(X_w = \sigma) = 1$ for all $w \in N_v \setminus \{u\}$, $P(X_{u'} = \sigma) = 0$ and $P(X_{w'} = \sigma) = 1$ for all $w' \in N_{v'} \setminus \{u'\}$. Since $\langle (u,v),(u',v') \rangle \in \mathcal{J}_{\mathsf{B/P}}$ we have $u' \in N_v \setminus \{u\}$ or $u \in N_{v'} \setminus \{u'\}$, leading to a contradiction. ∎

Lemma 4. *Consider the* B/M *model and let* $\mathcal{J}_{\mathsf{B/M}}$*, a set of unorderded pairs of* E*, be defined as*

$$\Big\langle (u,v),(u',v') \Big\rangle \in \mathcal{J}_{\mathsf{B/M}} \quad \textit{iff} \quad u' = v \textit{ or } u = v'. \tag{27}$$

Consider arbitrary subsets $U, W, U', W' \subseteq V$ *and assume* $\langle (u,v),(u',v') \rangle \in \mathcal{J}_{\mathsf{B/M}}$*. There does not exist a joint distribution on* X^V *satisfying* $P(X_w = \sigma) \in \{0,1\}$ *for all* $w \in V$ *such that both* $I(X_u; Y_v | X^U, Y^W) > 0$ *and* $I(X_{u'}; Y_{v'} | X^{U'}, Y^{W'}) > 0$.

Proof: Assume $I(X_u; Y_v | X^U, Y^W) > 0$ and $I(X_{u'}; Y_{v'} | X^{U'}, Y^{W'}) > 0$. By (3) and (8) we have $P(X_u = \sigma) = 0$, $P(X_v = \sigma) = 1$, $P(X_{u'} = \sigma) = 0$ and $P(X_{v'} = \sigma) = 1$. Since $\langle (u,v),(u',v') \rangle \in \mathcal{J}_{\mathsf{B/M}}$ we have $u' = v$ or $u = v'$, leading to a contradiction. ∎

The constraint graphs, as defined by (12), (19), (26) and (27), are illustrated in Figs. 4 and 5 for the line and hexagonal network respectively. Since the constraint graphs for the hexagonal network have many edges, we will not draw these graphs. Instead we will illustrate the constraint graphs as done in Fig. 5, or, for instance, by presenting sets of edges that form a clique in a constraint graph. It will be shown in the next two subsections that the transport capacity can be upper bounded in terms of the number of edges (u,v) in the graph (V,E) for which $I(X_u; Y_v)$ can be simultaneously positive. By Lemmas 1–4 it follows that this number is the size of the maximum independent set in the constraint graphs. Remember that an independent set of a graph is a set of vertices, no two of which are adjacent [34]. Since finding the size of the maximum independent set is a NP-complete problem [35], we will

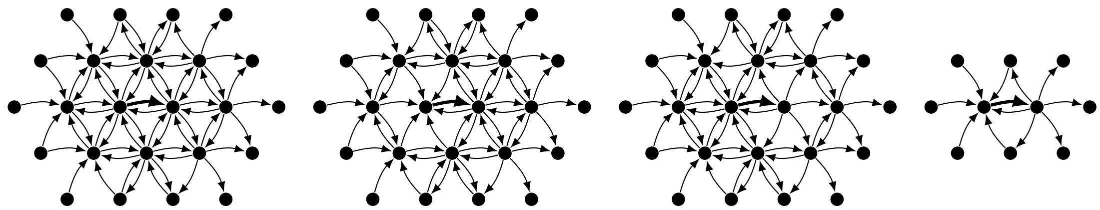

(a) P/P (b) B/P (c) P/M (d) B/M

Fig. 5. Illustration of the constraint graphs of the hexagonal network under the various models. In thin lines the edges that interfere with the thick edge, *i.e.*, in thin lines the set of edges (u', v') for which $\langle (u,v),(u',v')\rangle$ is in the constraint graph, where (u,v) is the thick edge.

derive upper bounds on this size. Note, finally, that our constraint graphs are very similar to the conflict graph, introduced in [36], where upper bounds are derived for multi-commodity flow problems in which network coding is not allowed.

A careful look at the constraint graphs of the line and hexagonal networks provides some intuition on the fact that the combined effects of multiaccess and broadcast are larger than the sum of their individual contributions, as observed in Section IV. We observe that $(E, \mathcal{J}_{\mathsf{B/P}})$ and $(E, \mathcal{J}_{\mathsf{P/M}})$ are subgraphs of $(E, \mathcal{J}_{\mathsf{P/P}})$. However, taking the intersection of $(E, \mathcal{J}_{\mathsf{B/P}})$ and $(E, \mathcal{J}_{\mathsf{P/M}})$ does not give $(E, \mathcal{J}_{\mathsf{B/M}})$. Therefore, the effect of exploiting both superposition and broadcast is larger than their individual contributions. The constraint graphs also provide some intuition on why the benefit in the hexagonal network is larger than in the line network. If we compare the ratio of the number of edges in $(E, \mathcal{J}_{\mathsf{P/P}})$ and $(E, \mathcal{J}_{\mathsf{B/M}})$, we see that this difference is much larger for the hexagonal network. Hence, larger benefits can be expected in the hexagonal network.

B. Line Network

The following lemma establishes the upper bound of Theorem 4.

Lemma 5. *The transport capacity $C^{\mathrm{line}}_{\mathsf{B/M}}(L)$ of the $L+1$ node line network under the* B/M *model is upper bounded by*

$$C^{\mathrm{line}}_{\mathsf{B/M}}(L) \leq L.$$

Proof: Let a set of unicast sessions and a network coding strategy over T time slots achieving rate R_k for session $k = 1, \dots, K$, be given. For $i = 0, \dots, L-1$, let $\Gamma_i = \{0, \dots, i\}$, $\bar{\Gamma}_i = \{i+1, \dots, L\}$, and $\mathcal{S} = \{\Gamma_i, \bar{\Gamma}_i | i = 0, \dots, L-1\}$. Since a unicast session over d hops crosses d cuts from $\mathcal{S}$,

$$\sum_{S \in \mathcal{S}} \sum_{k \in K_S} R_k = \sum_{k=1}^{K} \mathrm{dist}(S_k, D_k) R_k. \tag{28}$$

We start developing a cut-set bound following the line of proof found in [37, Theorem 14.10.1], for instance.

This gives

$$\sum_{k\in K_{\Gamma_i}} R_k \le \frac{1}{T}\sum_{t=1}^{T} I(X^{\Gamma_i}[t]; Y^{\bar{\Gamma}_i}[t]|X^{\bar{\Gamma}_i}[t]). \tag{29}$$

Summing the LHS and RHS in (29) over all $2L$ cuts in $\mathcal{S}$ and using (28) give

$$\sum_{k=1}^{K}\mathrm{dist}(S_k,D_k)R_k \le \frac{1}{T}\sum_{t=1}^{T}\sum_{i=0}^{L-1}[I(X^{\Gamma_i}[t];Y^{\bar{\Gamma}_i}[t]|X^{\bar{\Gamma}_i}[t]) + I(X^{\bar{\Gamma}_i}[t];Y^{\Gamma_i}[t]|X^{\Gamma_i}[t])], \tag{30}$$

where the second term on the RHS corresponds to reverse cuts $\bar{\Gamma}_i$. Now, due to the fact that the transmission schedule is fixed ahead of time, $P(X_v[t]=\sigma)\in\{0,1\}$ for each t and each $v\in V$. We proceed by upper bounding the RHS.

$$\sum_{k=1}^{K}\mathrm{dist}(S_k,D_k)R_k \le \max_t \sum_{i=0}^{L-1}[I(X^{\Gamma_i}[t];Y^{\bar{\Gamma}_i}[t]|X^{\bar{\Gamma}_i}[t]) + I(X^{\bar{\Gamma}_i}[t];Y^{\Gamma_i}[t]|X^{\Gamma_i}[t])]. \tag{31}$$

This means, that for any achievable transport capacity, there must exist a joint distribution on X_v, with $P(X_v = \sigma)\in\{0,1\}$ for each $v\in V$, satisfying

$$\sum_{k=1}^{K}\mathrm{dist}(S_k,D_k)R_k \le \sum_{i=0}^{L-1}[I(X^{\Gamma_i};Y^{\bar{\Gamma}_i}|X^{\bar{\Gamma}_i}) + I(X^{\bar{\Gamma}_i};Y^{\Gamma_i}|X^{\Gamma_i})] \tag{32}$$

$$\le \sum_{i=0}^{L-1}[I(X_i;Y_{i+1}|X^{\bar{\Gamma}_i}) + I(X_{i+1};Y_i|X^{\Gamma_i})], \tag{33}$$

where the second inequality follows after decomposing the mutual information terms and using (8).[2]

We now argue that for all probability distributions of this kind, the right hand side of (33) is upper bounded by L. From (8) it follows that each term individually can be at most one. Therefore, it is sufficient to show that at most L terms in (33) can be made positive. By Lemma 4, this number is exactly the size of the maximum independent set in the constraint graph $(E,\mathcal{J}_{\mathsf{B/M}})$, which is depicted in Fig. 6(a). Since the size of the maximum independent set can not decrease in size by removing some of the edges of $(E,\mathcal{J}_{\mathsf{B/M}})$, we consider the graph given in 6(b). Since this graph consists of disjoint components which are cliques, the maximum independent set is upper bound by the number of components, which is L. ■

The following lemma establishes the upper bound of Theorem 2.

Lemma 6. *The transport capacity $C^{\mathrm{line}}_{\mathsf{B/P}}(L)$ of the $L+1$ node line network under the* B/P *model is upper bounded by*

$$C^{\mathrm{line}}_{\mathsf{B/P}}(L) \le \left\lceil \frac{2}{3}L \right\rceil.$$

Proof: We apply Lemma 3 by starting from (33) and considering the constraint graph $(E,\mathcal{J}_{\mathsf{B/P}})$ as given in Fig. 6(c). Again, by removing edges we get the graph depicted in Fig. 6(d), which consists of disjoint components

[2]A more common form of the cut-set bound is to introduce a time-sharing variable and perform an averaging argument instead of taking the maximum over t on the RHS. In general, however, the averaged distribution does not satisfy the condition that $P(X_v=\sigma)\in\{0,1\}$ for all $v\in V$.

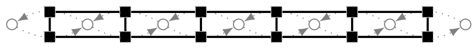

(a) Constraint graph $(E, \mathcal{J}_{\mathsf{B/M}})$ for the line network, where E is represented by square shaped nodes and $\mathcal{J}_{\mathsf{B/M}}$ by solid lines. Moreover, the line network (V, E) is depicted by circle shaped nodes and dotted lines.

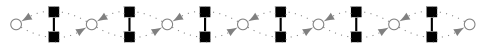

(b) $(E, \mathcal{J}')$, where $\mathcal{J}' \subset \mathcal{J}_{\mathsf{B/M}}$.

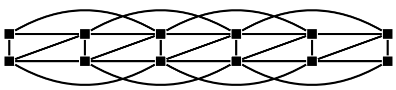

(c) Constraint graph $(E, \mathcal{J}_{\mathsf{B/P}})$ for the line network. (V, E) is now omitted for clarity.

(d) $(E, \mathcal{J}')$, where $\mathcal{J}' \subset \mathcal{J}_{\mathsf{B/P}}$.

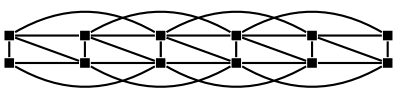

(e) Constraint graph $(E, \mathcal{J}_{\mathsf{P/M}})$ for the line network.

(f) $(E, \mathcal{J}')$, where $\mathcal{J}' \subset \mathcal{J}_{\mathsf{P/M}}$.

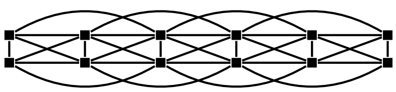

(g) Constraint graph $(E, \mathcal{J}_{\mathsf{P/P}})$ for the line network.

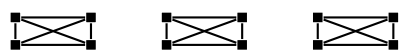

(h) $(E, \mathcal{J}')$, where $\mathcal{J}' \subset \mathcal{J}_{\mathsf{P/P}}$.

Fig. 6. Line network. Interference relations under different communication models.

which are cliques. In counting the number of cliques we need to take into account edge effects. It can easily be verified that we have $2\left\lfloor \frac{L}{3} \right\rfloor + (L \bmod 3) = \left\lceil \frac{2L}{3} \right\rceil$ cliques. ■

The following lemma establishes the upper bound of Theorem 3.

Lemma 7. *The transport capacity $C^{\text{line}}_{\mathsf{P/M}}(L)$ of the $L+1$ node line network under the* P/M *model is upper bounded by*

$$C^{\text{line}}_{\mathsf{P/M}}(L) \leq \left\lceil \frac{2}{3} L \right\rceil .$$

Proof: We apply Lemma 2 by starting from (33) and considering the constraint graph $(E, \mathcal{J}_{\mathsf{P/M}})$ as given in Fig. 6(e). Again, by removing edges we get the graph depicted in Fig. 6(f), which consists of disjoint components which are cliques. Now, by similarity to Fig. 6(d), the size of the maximum independent set equals that of the B/P case. ■

The following lemma establishes the upper bound of Theorem 1.

Lemma 8. *The transport capacity $C^{\text{line}}_{\mathsf{P/P}}(L)$ of the $L+1$ node line network under the* $\mathsf{P/P}$ *model is upper bounded by*

$$C^{\text{line}}_{\mathsf{P/P}}(L) \leq \left\lceil \frac{1}{2} L \right\rceil .$$

Proof: We apply Lemma 1 by starting from (33) and considering the constraint graph $(E, \mathcal{J}_{\mathsf{P/P}})$ as given in Fig. 6(g). Again, by removing links we get the graph depicted in Fig. 6(h), which consists of disjoint components which are cliques. It can easily be verified that we have $\left\lfloor \frac{L}{2} \right\rfloor + (L \bmod 2) = \left\lceil \frac{L}{2} \right\rceil$ cliques. ■

C. Hexagonal Lattice

In this section we establish the upper bounds of Theorems 5–8. The following lemma establishes the upper bound of Theorem 8.

Lemma 9. *The transport capacity $C^{\text{hex}}_{\mathsf{B/M}}(L, M)$ of the $(L+1) \times (M+1)$ node hexagonal network under the* $\mathsf{B/M}$ *model is upper bounded by*

$$C^{\text{hex}}_{\mathsf{B/M}}(L, M) \leq 2LM + 2(L + M).$$

Proof: Consider the cuts

$$\Gamma^1_i = \{(u_1, u_2) \in V | u_1 \leq i\}, \quad i = 0, \ldots, L-1, \tag{34}$$

$$\Gamma^2_i = \{(u_1, u_2) \in V | u_2 \leq i\}, \quad i = 0, \ldots, M-1, \tag{35}$$

$$\Gamma^3_i = \{(u_1, u_2) \in V | u_1 + u_2 \leq i\}, \quad i = 0, \ldots, L+M-1. \tag{36}$$

Let

$$\mathcal{S} = \{\Gamma^1_i, \bar{\Gamma}^1_i\}_{i=0}^{L-1} \cup \{\Gamma^2_i, \bar{\Gamma}^2_i\}_{i=0}^{M-1} \cup \{\Gamma^3_i, \bar{\Gamma}^3_i\}_{i=0}^{L+M-1}, \tag{37}$$

where we have used the notation $\bar{\Gamma}^j_i = V \setminus \Gamma^j_i$. Fig. 7 depicts (V, E) and the lines inducing the cuts in $\mathcal{S}$.

Since on the shortest path between two nodes, the number of cuts crossed on each hop is 2 and no cut is crossed more than once,

$$\sum_{S \in \mathcal{S}} \sum_{k \in K_S} R_k = 2 \sum_{k=1}^{K} \text{dist}(S_k, D_k) R_k. \tag{38}$$

Developing a cut-set bound in similar fashion to the proof of Lemma 5 and summing over all cuts leads to

$$2 \sum_{k=1}^{K} \text{dist}(S_k, D_k) R_k \leq \sum_{i=0}^{L-1} [I(X^{\Gamma^1_i}; Y^{\bar{\Gamma}^1_i} | X^{\bar{\Gamma}^1_i}) + I(X^{\bar{\Gamma}^1_i}; Y^{\Gamma^1_i} | X^{\Gamma^1_i})] \tag{39}$$

$$+ \sum_{i=0}^{M-1} [I(X^{\Gamma^2_i}; Y^{\bar{\Gamma}^2_i} | X^{\bar{\Gamma}^2_i}) + I(X^{\bar{\Gamma}^2_i}; Y^{\Gamma^2_i} | X^{\Gamma^2_i})] \tag{40}$$

$$+ \sum_{i=0}^{L+M-1} [I(X^{\Gamma^3_i}; Y^{\bar{\Gamma}^3_i} | X^{\bar{\Gamma}^3_i}) + I(X^{\bar{\Gamma}^3_i}; Y^{\Gamma^3_i} | X^{\Gamma^3_i})], \tag{41}$$

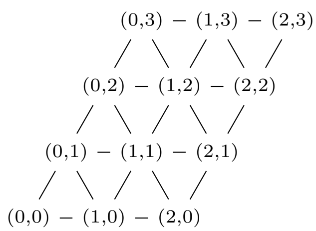

(a) Hexagonal network (V, E) for $L = 2$, $M = 3$.

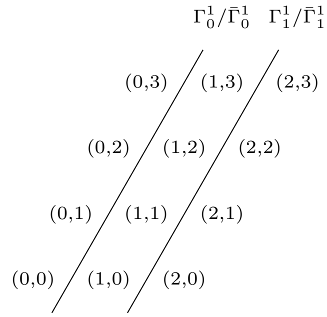

(b) Lines inducing the partitions Γ_i^1 and $\bar{\Gamma}_i^1$, $i = 0, \dots, L-1$.

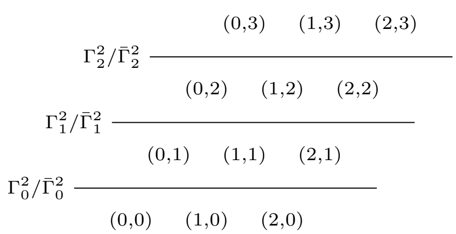

(c) Lines inducing the partitions Γ_i^2 and $\bar{\Gamma}_i^2$, $i = 0, \dots, M-1$.

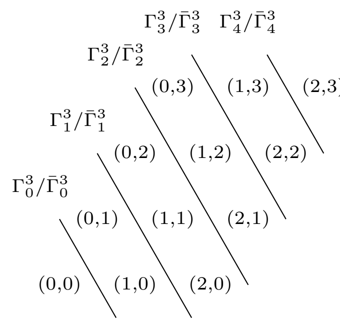

(d) Lines inducing the partitions Γ_i^3 and $\bar{\Gamma}_i^3$, $i = 0, \dots, L+M-1$.

Fig. 7. Hexagonal network with vertices located at the hexagonal lattices and edges between nearest neighbours. Moreover, lines inducing the cuts used to upper bound its transport capacity.

which is the equivalent of (32). By decomposing the mutual information terms on the RHS we obtain

$$\sum_{k=1}^{K} \text{dist}(S_k, D_k) R_k \leq \frac{1}{2} \sum_{(u,v) \in E} \left[I(X_u; Y_v | X^{A(u,v)}, Y^{B(u,v)}) + I(X_v; Y_u | X^{C(u,v)}, Y^{D(u,v)}) \right]. \tag{42}$$

The sets $A(u,v)$, $B(u,v)$, $C(u,v)$ and $D(u,v)$ capture the conditioning terms. We will apply Lemma 4 which does not depend on the conditioning. Therefore, these sets do not affect the remainder and we will leave them unspecified. From (42) and Lemma 4 it follows that the transport capacity is upper bounded by the size of the maximum independent set in the constraint graph $(E, \mathcal{J}_{\mathsf{B/M}})$. Note that any 3-cycle in the hexagonal network (V, E) forms a clique in the constraint graph $(E, \mathcal{J}_{\mathsf{B/M}})$. Therefore, we construct a set $\mathcal{J}' \subset \mathcal{J}_{\mathsf{B/M}}$ consisting of 3-cycles and some unconnected nodes. Fig. 8 depicts $\mathcal{J}'$. It can be readilly verified that there are $2LM$ cycles and $2(L+M)$ unconnected nodes. Therefore, the size of the maximum independent set is upper bounded by $2LM + 2(L+M)$. ∎

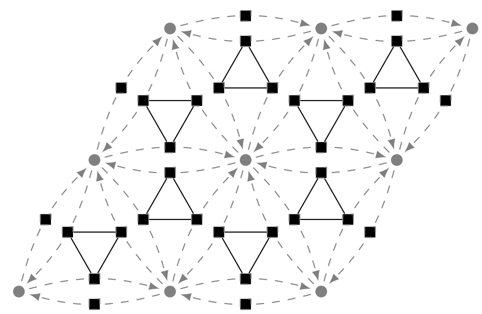

Fig. 8. Subgraph of the constraint graph $(E, \mathcal{J}_{\mathsf{B/M}})$. Depicted are $(E, \mathcal{J}')$, $\mathcal{J}' \subset \mathcal{J}_{\mathsf{B/M}}$, with E as square vertices and $\mathcal{J}'$ as solid lines and the hexagonal network (V, E) in round vertices and dashed lines.

The following lemma establishes the upper bound of Theorem 7.

Lemma 10. *The transport capacity $C^{\text{hex}}_{\mathsf{B/P}}(L, M)$ of the $(L+1) \times (M+1)$ node hexagonal network under the* B/P *model is upper bounded by*

$$C^{\text{hex}}_{\mathsf{B/P}}(L, M) \leq \frac{6}{7} LM + \mathrm{o}(LM).$$

Proof: We use the same line of proof as used for Lemma 9. The set of edges depicted in Fig. 9(a) form a clique in the constraint graph $(E, \mathcal{J}_{\mathsf{B/P}})$. Fig. 9 illustrates that based on this clique the size of the maximum independent set of $(E, \mathcal{J}_{\mathsf{B/P}})$ can be upper bounded by $\frac{6}{7} LM + \mathrm{o}(LM)$. In Fig. 9(c) six cliques from Fig. 9(a) are depicted. In Fig. 9(d) the resulting graph is tiled around the hexagonal network, ensuring that all edges are covered exactly once. ■

The following lemma establishes the upper bound of Theorem 6.

Lemma 11. *The transport capacity $C^{\text{hex}}_{\mathsf{P/M}}(L, M)$ of the $(L+1) \times (M+1)$ node hexagonal network under the* P/M *model is upper bounded by*

$$C^{\text{hex}}_{\mathsf{P/M}}(L, M) \leq \frac{6}{7} LM + \mathrm{o}(LM).$$

Proof: This results follows using the proof of Lemma 10 with the edges from Fig. 9(b) as a clique and a tiling of cliques as depicted in Fig. 9. ■

The following lemma establishes the upper bound of Theorem 5.

Lemma 12. *The transport capacity $C^{\text{hex}}_{\mathsf{P/P}}(L, M)$ of the $(L+1) \times (M+1)$ node hexagonal network under the* P/P *model is upper bounded by*

$$C^{\text{hex}}_{\mathsf{P/P}}(L, M) \leq \frac{2}{5} LM + \mathrm{o}(LM).$$

Proof: Again, we use the same line of proof as used for Lemma 9. Consider the set of edges depicted in Fig. 10(a). The set is partitioned in two, such that the edges in each partition form a clique in the constraint graph $(E, \mathcal{J}_{\mathsf{P/P}})$. This means that the size of the maximum independent set of this subset of $(E, \mathcal{J}_{\mathsf{P/P}})$ is 2. Also, the set

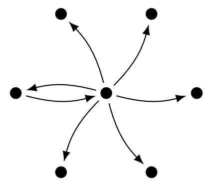

(a) Clique in $(E, \mathcal{J}_{\mathsf{B/P}})$.

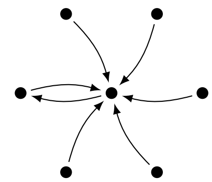

(b) Clique in $(E, \mathcal{J}_{\mathsf{P/M}})$.

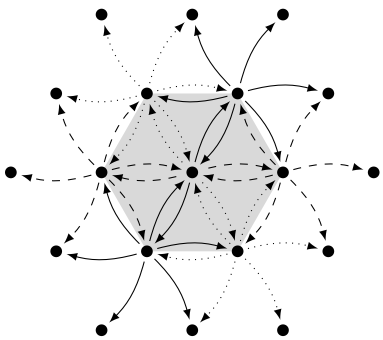

(c) Six cliques as given in (a)

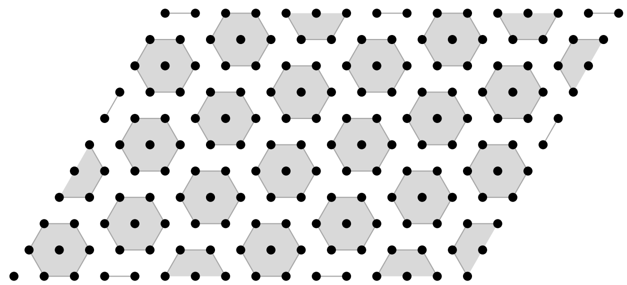

(d) Tiling the structure from (c).

Fig. 9. Subgraphs of the hexagonal network such that the edges form a clique in the constraint graph $(E, \mathcal{J}_{\mathsf{B/P}})$ and $(E, \mathcal{J}_{\mathsf{P/M}})$ respectively.

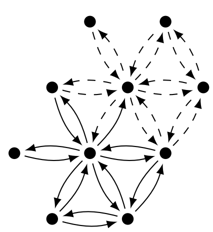

(a) Two cliques of $(E, \mathcal{J}_{\mathsf{P/P}})$.

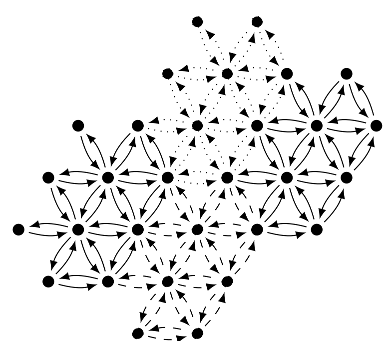

(b) Tiling the structure of (a).

Fig. 10. Subgraphs of the hexagonal network for which the edges form a clique in the constraint graph $(E, \mathcal{J}_{\mathsf{P/P}})$.

of edges from Fig. 10(a) can be tiled around in such a way that all edges in (V, E) are covered exactly once. This is depicted in Fig. 10(b). From Fig. 10(b) it is clear that the number of times that the set from Fig. 10(a) is used in the tiling is $LM/5 + \mathrm{o}(LM)$. Hence the size of the maximum independent set is at most $\frac{2}{5}LM + \mathrm{o}(LM)$. ■

VI. Achievable Schemes

A. Line Network

In this section we establish the lower bounds of Theorems 1–4. The following lemma establishes the lower bound of Theorem 4.

Lemma 13. *The transport capacity $C^{\text{line}}_{\mathsf{B/M}}(L)$ of the $L+1$ node line network under the* $\mathsf{B/M}$ *model satisfies*

$$C^{\text{line}}_{\mathsf{B/M}}(L) \geq L.$$

Proof: We consider the multiple unicast configuration in which two sessions have sources and receivers at the endpoints of the network, *i.e.*,

$$\begin{aligned} S_1 = 0, \quad D_1 = L, \\ S_2 = L, \quad D_2 = 0. \end{aligned} \tag{43}$$

Let $\{m[t]\}$ and $\{\bar{m}[t]\}$ be the sequence of source symbols transmitted by S_1 and S_2 respectively. We will show that the nodes in the network are able to operate in such a fashion that the symbols transmitted are as depicted in Fig. 11.

Communication proceeds in rounds. Each round consists of two time slots. In the first time slot the even nodes transmit; in the second time slot the odd nodes transmit. Round 0 starts at time slot 0. Let $\tilde{x}_i[r]$ be the symbol transmitted by node i in round r. This gives

$$x_i[t] = \begin{cases} \tilde{x}_i[\lfloor t/2 \rfloor], & \text{if } t \equiv i \pmod 2 \\ \sigma, & \text{otherwise.} \end{cases} \tag{44}$$

Note, that each node receives one useful symbol in each round. Each node is transmitting in one of the time slots in each round and is not able to receive due to half-duplex constraints. Let $\tilde{y}_i[r]$ denote the symbol received by node i in round r. It is readilly verified that $\tilde{y}_i[r] = \tilde{x}_{i-1}[r]\mathbf{1}_{\{i>0\}} + \tilde{x}_{i+1}[r]\mathbf{1}_{\{i<L\}}$.

Now we specify what symbols $\tilde{x}_i[r]$ are transmitted. In round 0 the only non-zero symbols that are transmitted are $\tilde{x}_0[0] = m[0]$ and $\tilde{x}_L[0] = \bar{m}[0]$. In the next rounds coding occurs as follows

$$\tilde{x}_i[r] = \begin{cases} m[r] + \bar{m}[r-L], & \text{if } i = 0, \\ \tilde{y}_i[r-1] - \tilde{x}_i[r-2], & \text{if } 0 < i < L, \\ \bar{m}[r] + m[r-L], & \text{if } i = L, \end{cases} \tag{45}$$

with the convention that $m[r-L]$ and $\bar{m}[r-L]$ are 0 for $r < L$. Note, that it is implied by (45), that node 0 (L), which is the receiver R_1 (R_2), has properly decoded source symbol $\bar{m}[r-L]$ ($m[r-L]$) before starting round r. We will need to verify that the receivers are actually able to decode. Using induction over the rounds, however, we can easily verify that

$$\tilde{x}_i[r] = m[r-i] + \bar{m}[r-L+i], \tag{46}$$

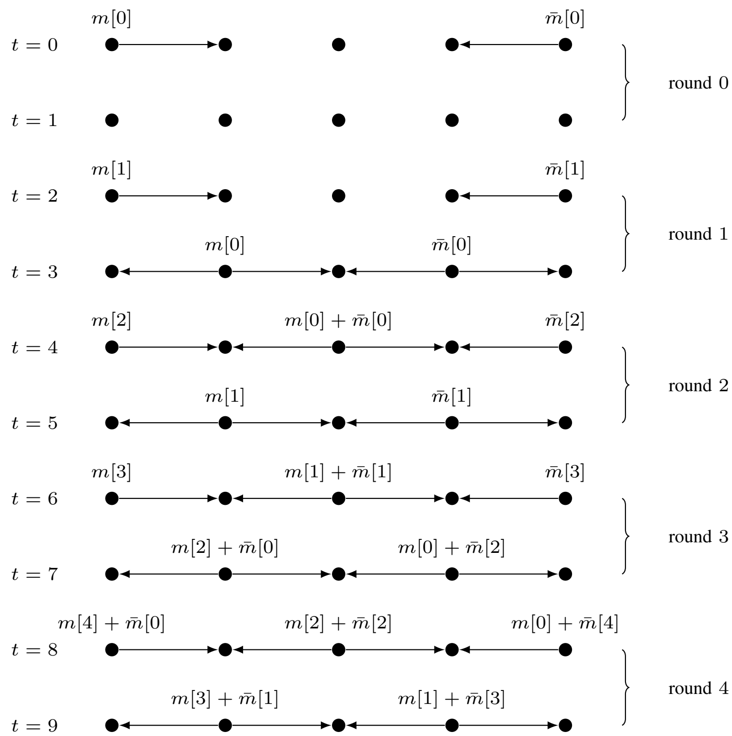

Fig. 11. Demonstration of the achievable scheme on the line network under B/M.

as also reflected in Fig. 11.

The decoding procedure for $\bar{m}[r-L]$ by node 0 at the end of round $r-1$ is

$$\bar{m}[r-L] = \tilde{y}_0[r-1] - m[r-2], \tag{47}$$

which follows by $\tilde{y}_0[r-1] - m[r-2] = \tilde{x}_1[r-1] - m[r-2] = m[r-2] + \bar{m}[r-L] - m[r-2] = \bar{m}[r-L]$. In similar fashion it follows that the decoding procedure for $m[r-L]$ by node L at the end of round $r-1$ is

$$m[r-L] = \tilde{y}_L[r-1] - \bar{m}[r-2]. \tag{48}$$

In each round one symbol for each session is transmitted and successfully decoded some rounds later. The number of time slots per session is 2. Hence, the throughput for both sessions equals $1/2$. For each session we have $|S_k - D_k| = L$, hence the transport capacity is lower bounded by L. ∎

The following lemma establishes the lower bound of Theorem 2.

Lemma 14. *The transport capacity $C^{\text{line}}_{\mathsf{B/P}}(L)$ of the $L+1$ node line network under the* B/P *model satisfies*

$$C^{\text{line}}_{\mathsf{B/P}}(L) \geq \frac{2}{3}L.$$

Proof: We consider the same multiple unicast configuration as used in the proof of Lemma 13, *i.e.*, according to (43), with two sessions that have sources and receivers at the endpoints of the network. Many elements, in

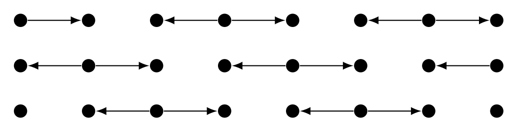

Fig. 12. Transmission schedule for one round in the achievable scheme for the line network under $\mathsf{B/P}$.

particular notation, of the proof are the same as the proof of Lemma 13. The scheme operates in rounds of *three* time slots. Again operation is such that each node is transmitting exactly once in each round, *i.e.*,

$$x_i[t] = \begin{cases} \tilde{x}_i[\lfloor t/3 \rfloor], & \text{if } t \equiv i \pmod 3, \\ \sigma, & \text{otherwise,} \end{cases} \tag{49}$$

where $\tilde{x}_i[r]$ is the symbol transmitted by node i in round r. The scheduling is illustrated in Fig. 12. As a consequence of (49) each node that is not at the border of the network receives two symbols in each round. Let $\tilde{y}_i[r]$ denote the sum (over $\mathbb{F}_q$) of the received symbols. Now, we proceed along the lines of the proof of Lemma 13: coding is according to (45) and relations (46), (47) and (48) hold. Hence, the two sessions achieve throughput $\frac{1}{3}$ symbols per time slot over distance L, leading to a lower bound of $\frac{2}{3}L$ symbols×hops per time slot on the transport capacity. ■

The scheme given for the proof of Lemma 14 is essentially the same as used for the proof of Lemma 13. The main difference is in the scheduling of the transmissions. The next lemma provides the lower bound required for Theorem 3. Again the scheme is essentially the same as in the above two lemmas.

Lemma 15. *The transport capacity $C^{\text{line}}_{\mathsf{P/M}}(L)$ of the $L+1$ node line network under the $\mathsf{P/M}$ model satisfies*

$$C^{\text{line}}_{\mathsf{P/M}}(L) \geq \frac{2}{3}L.$$

Proof: We continue with the configuration and notation used in the proof of Lemmas 13 and 14. Rounds consist of three time slots, with node i transmitting the symbol $\tilde{x}_i[r]$ in round r. More precisely, we have

$$x_i[t] = \begin{cases} \tilde{x}_i[\lfloor t/3 \rfloor], & \text{if } (i-t) \equiv 0 \pmod 3 \text{ and } i > 0, \\ \tilde{x}_i[\lfloor t/3 \rfloor], & \text{if } (i-t) \equiv 1 \pmod 3 \text{ and } i < L, \\ \sigma, & \text{otherwise.} \end{cases} \tag{50}$$

Note that this means that nodes $1, \dots, L-1$ transmit the same symbol twice in each round. Nodes 0 and L transmit only once. Let $a_i[t]$ denote the neighbour that i is transmitting to in time slot t. We need to define $a_i[t]$ only for those time slots in which a node is transmitting. We use

$$a_i[t] = \begin{cases} i-1, & \text{if } (i-t) \equiv 0 \pmod 3, \\ i+1, & \text{if } (i-t) \equiv 1 \pmod 3, \end{cases} \tag{51}$$

leading to the transmission schedule depicted in Fig. 13. Now we perform coding and decoding according to (45)–(48). Since rounds consist of three time slots, we achieve $\frac{2}{3}L$ symbols×hops per time slot. ■

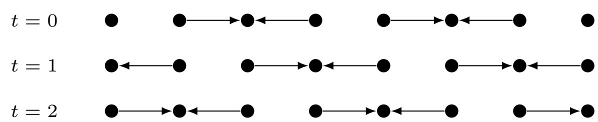

Fig. 13. Transmission schedule for one round in the achievable scheme for the line network under $\mathsf{P/M}$.

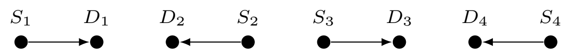

Fig. 14. Configuration of unicast sessions, used to achieve $\lceil L/2 \rceil$ symbols$\times$hops per time slot under $\mathsf{P/P}$.

The following lemma establishes the lower bound of Theorem 1.

Lemma 16. *The transport capacity $C^{\text{line}}_{\mathsf{P/P}}(L)$ of the $L+1$ node line network under the $\mathsf{P/P}$ model satisfies*

$$C^{\text{line}}_{\mathsf{P/P}}(L) \geq \left\lceil \frac{1}{2} L \right\rceil .$$

Proof: Let unicast sessions be given as depicted in Fig. 14. The number of sessions equals $\lceil L/2 \rceil$. The sources of all sessions can transmit simultaneously without causing interference. Therefore, the number of symbols$\times$hops per time slot that is achieved equals the number of sessions, $\lceil L/2 \rceil$. No (de)coding is required since all sinks receive uncoded information directly from their source. ■

B. Hexagonal Lattice

In this section we give constructive schemes on the hexagonal lattice, providing proofs for the achievable part of Theorems 5–8. The next lemma provides the lower bound required for Theorem 5.

Lemma 17. *The transport capacity $C^{\text{hex}}_{\mathsf{P/P}}(L, M)$ of the $(L+1) \times (M+1)$ node hexagonal network under the $\mathsf{P/P}$ model satisfies*

$$C^{\text{hex}}_{\mathsf{P/P}}(L, M) \geq \frac{1}{3} LM + \mathrm{o}(LM).$$

Proof: Let unicast sessions be given as depicted in Fig. 15. The number of sessions equals $LM/3 + \mathrm{o}(LM)$. The sources of all sessions can transmit simultaneously without causing interference at the destinations. Therefore, the number of symbols$\times$hops per time slot that is achieved equals the number of sessions, $LM/3 + \mathrm{o}(LM)$. No (de)coding is required since all sinks receive uncoded information directly from their source. ■

The next lemma provides the lower bound required for Theorem 7.

Lemma 18. *The transport capacity $C^{\text{hex}}_{\mathsf{B/P}}(L, M)$ of the $(L+1) \times (M+1)$ node hexagonal network under the $\mathsf{B/P}$ model is at least*

$$C^{\text{hex}}_{\mathsf{B/P}}(L, M) \geq \frac{2}{5} L(M+1).$$

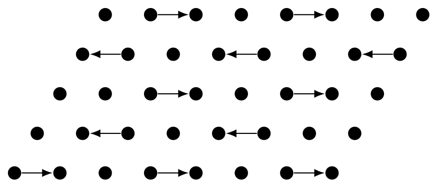

Fig. 15. Configuration of unicast sessions on the hexagonal lattice, used to achieve $LM/3 + \mathrm{o}(LM)$ symbols×hops per time slot under P/P.

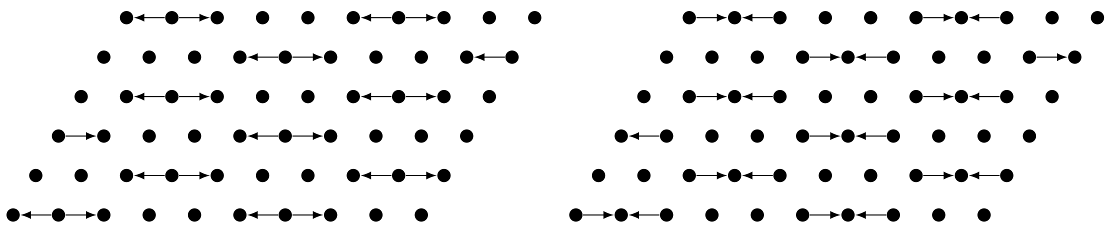

(a) B/P (b) P/M

Fig. 16. A valid scheduling of transmissions under the B/P and P/M models.

Proof: Consider $2(M+1)$ unicast sessions with sources and sinks at the left and right borders of the network, *i.e.*, $S_k = (0,k)$, $D_k = (L,k)$ for $k = 0,\dots,M$ and $S_{\bar{k}} = \big(L,\bar{k}\big)$, $D_{\bar{k}} = \big(0,\bar{k}\big)$ for $\bar{k} = M+1,\dots,2M+1$. Consider a scheduling of transmissions as depicted in Fig. 16(a). By using 5 time slots and shifting this pattern of scheduled transmissions around, each node is transmitting to its left and right neighbour exactly once in each round. Now, using the scheme given in the proof of Lemma 14, we achieve a throughput of $1/5$ for each session. In total there are $2(M+1)$ sessions over distance L. ■

The next lemma provides the lower bound required for Theorem 6.

Lemma 19. *The transport capacity* $C^{\mathrm{hex}}_{\mathsf{P/M}}(L,M)$ *of the* $(L+1)\times(M+1)$ *node hexagonal network under the* P/M *model satisfies*

$$C^{\mathrm{hex}}_{\mathsf{P/M}}(L,M) \geq \frac{2}{5}L(M+1).$$

Proof: The proof is along the lines of the proof of Lemma 18, but with a scheduling as depicted in Fig. 16(b) and the line network coding scheme from Lemma 15. ■

Note that in the previous two lemmas we can also achieve $\frac{2}{5}(L+1)M$ by considering sessions from top to bottom and vice versa. Both lead to $\frac{2}{5}LM + \mathrm{o}(LM)$ symbols×hops per time slot as given in the statement of Theorems 6 and 7.

Finally we present an achievable scheme for the B/M model, providing a proof for the lower bound of Theorem 8. The achievable scheme for the B/M model is constructed based on a simple transmission scheme, consisting of the following elements:

Even-odd scheduling: Transmissions are scheduled in such a way that node (u_1,u_2) transmits in time slot t

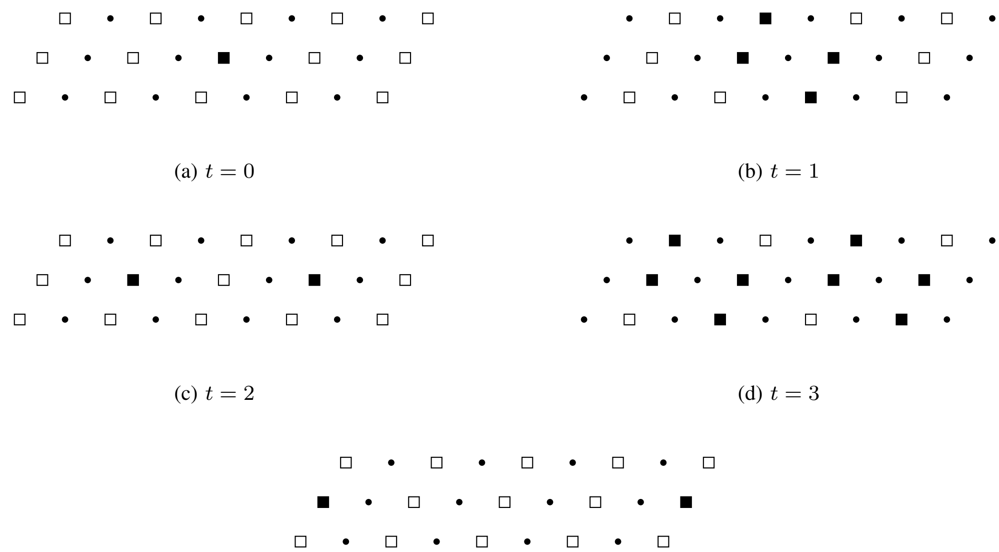

(a) $t = 0$ (b) $t = 1$

(c) $t = 2$ (d) $t = 3$

(e) $t = 4$

Fig. 17. Illustrating even-odd scheduling and simple retransmissions over $\mathbb{F}_2$ under B/M. Nodes that are transmitting are depicted by square vertices. Filled vertices are transmitting a symbol, other vertices transmit zero.

iff $u_1 \equiv t \pmod 2$.

Simple retransmissions: All symbols are from $\mathbb{F}_2$. Nodes retransmit what they have received in the previous time slot. Since we operate under B/M this is the sum of what has been transmitted by its neighbours.

Even-odd scheduling and simple retransmissions are illustrated in Fig. 17 for the special case of $L = 8$ and $M = 2$. In the figure one can observe that a symbol that is initially transmitted by one node will be retransmitted four time slots later by exactly two other nodes. This is made precise in the following lemma which we will prove in Appendix A.

Lemma 20. *Assume even-odd scheduling and simple retransmissions over* $\mathbb{F}_2$ *on the* $(L+1) \times (M+1)$ *hexagonal network, where* $M = 2^\kappa - 2$, $\kappa \geq 2$ *and* $L \geq 2^{\kappa+1}$. *Let* $2^\kappa \leq u_1 \leq L - 2^\kappa$, *even, and* $0 \leq u_2 \leq M$. *Suppose that in time slot* $t = 0$ *node* (u_1, u_2) *transmits a symbol* m *and all other nodes transmit* 0. *Then, at time* $t = 2^\kappa$, *nodes* $(u_1 - 2^\kappa, u_2)$ *and* $(u_1 + 2^\kappa, u_2)$ *transmit* m *and all other nodes transmit* 0.

Note that the height of the network, *i.e.*, the value of M, is critical. The result does not hold for arbitrary values of M. Using the even-odd scheduling, the simple retransmission scheme and the above result we are now ready to prove the lower bound of Theorem 8.

Lemma 21. *Assume* $q = 2$. *The transport capacity* $C^{\mathrm{hex}}_{\mathsf{B/M}}(L, M)$ *of the* $(L+1) \times (M+1)$ *node hexagonal network* *under the* $\mathsf{B/M}$ *model satisfies*

$$C^{\text{hex}}_{\mathsf{B/M}}(L, M) \geq LM + \text{o}(LM).$$

Proof: Assume for the moment that

$$M = 2^\kappa - 2, \quad \text{and} \quad L = (a+2) \cdot 2^\kappa - 2, \tag{52}$$

for integers $\kappa \geq 2$ and $a \geq 1$. The network is operated in rounds of 2^κ time slots. In the first time slot of a round each node transmits according to a coding scheme that will be specified below. In the remaining time slots operation of the network is restricted to even-odd scheduling and simple retransmissions. The symbols that are received in the final time slot of a round are stored, the other symbols are discarded. From Lemma 20 and linearity of the coding operations it follows that employing even-odd scheduling and simple retransmissions decomposes the network into independent line networks that are operated in rounds of 2^κ time slots. More precisely, for each $0 \leq c_1 \leq 2^{\kappa-1} - 1$ and $0 \leq c_2 \leq 2^\kappa - 2$ we have an 'induced line network' consisting of the points

$$(2^\kappa + 2c_1, c_2), (2 \cdot 2^\kappa + 2c_1, c_2), (3 \cdot 2^\kappa + 2c_1, c_2), \ldots, (a \cdot 2^\kappa + 2c_1, c_2). \tag{53}$$

The choice of L in (52) comes from the fact that for point $(a \cdot 2^\kappa + 2^\kappa - 2, u_2)$ of the line network with $c_1 = 2^{\kappa-1} - 1$ and $c_2 = u_2$, we need

$$a \cdot 2^\kappa + 2^\kappa - 2 \leq L - 2^\kappa \tag{54}$$

in order to apply Lemma 20.

There are $2^{\kappa-1}(2^\kappa - 1)$ induced line networks, each of size a. Note, that these line networks do not have any half-duplex constraints. This means that for each induced line network, the achievable strategy used in Lemma 13 can be extended to a strategy in which all transmissions are scheduled simultaneously. For each 'induced line network' this leads to 2 sessions, each operating at throughput 1 symbol per round, transmitting over a distance of $a - 1$ 'induced hops'. Hence, each induced line network supports $2(a-1)$ symbols$\times$'induced hops' per round. Since the length of an induced hop is 2^κ, and the length of a round is 2^κ time slots, it follows that the capacity of the hexagonal network is lower bounded by

$$2(a-1)2^{\kappa-1}\,(2^\kappa - 1)\,2^\kappa 2^{-\kappa} = (a-1)2^\kappa(2^\kappa - 1) \tag{55}$$

symbols$\times$hops per time slot.

Finally, we relax constraint (52) and consider the case of arbitrary (large) L and M. The scheme that was developed above, will be applied to disjoint subsets of the network of size $(L'+1) \times (M'+1)$, where

$$M' = 2^\kappa - 2, \text{and } L' = (a+2) \cdot 2^\kappa - 2, \tag{56}$$

with

$$\kappa = \lfloor \log_2 \log_2(M+1) \rfloor, \tag{57}$$

and

$$a = \max\{a' \in \mathbb{N} \mid (a'+2)2^\kappa - 2 \leq L\} = \left\lfloor \frac{L+2}{2^\kappa} \right\rfloor - 2. \tag{58}$$

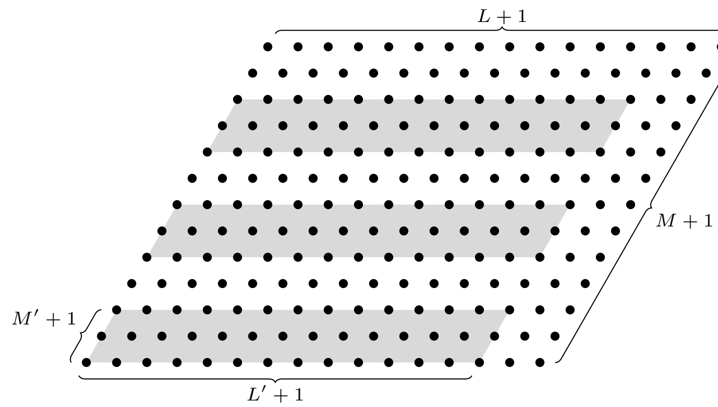

Fig. 18. Subsets of size $(L'+1)\times(M'+1)$.

These subsets are chosen in such a way that they are separated by one horizontal line of nodes that remain silent and are not used. The idea is depicted in Fig. 18. Note that the condition $M \geq 15$ ensures $\kappa \geq 2$. We observe that the number of subsets created equals

$$b = \left\lfloor \frac{M+1}{2^\kappa} \right\rfloor. \tag{59}$$

In each subset of size $(L'+1)\times(M'+1)$ the number of symbols×hops per time slot that is achieved is given by (55). Hence, combining (55), (57), (58) and (59), the number of symbols×hops per time slot that is achieved in the whole network of size $(L+1)\times(M+1)$ equals

$$\begin{aligned} b(a-1)2^\kappa\left(2^\kappa-1\right) &= \left\lfloor \frac{M+1}{2^\kappa} \right\rfloor \left(\left\lfloor \frac{L+2}{2^\kappa} \right\rfloor - 3 \right) 2^\kappa\left(2^\kappa-1\right) \\ &\geq \left(\frac{M+1}{2^\kappa}-1\right)\left(\frac{L+2}{2^\kappa}-4\right)2^\kappa\left(2^\kappa-1\right) \\ &= \left(M+1-2^\kappa\right)\left(L+2-2^{\kappa+2}\right)\left(1-2^{-\kappa}\right) \\ &\geq \left(M+1-\log_2(1+M)\right)\left(L+2-4\log_2(1+M)\right)\left(1-\frac{1}{\frac{1}{2}\log_2(1+M)}\right) \\ &= LM + \mathrm{o}(LM). \end{aligned}$$

■

VII. Extension to Gaussian Models

The main results of this work are Theorems 1–4 and 5–8 from Section IV. These results give bounds on the capacity of networks with a deterministic communication model, as defined in Section III. Our main results can be used to infer results for networks with more intricate communication models by a two-step procedure. In the first step, the more intricate communication model is reduced to one of the four deterministic models. This step will typically involve suitable error-correcting codes. In the second step, using the reduced network model, the results of this paper can be directly applied. In this section, we give an outline of this procedure for a simple Gaussian model with local interference.

A. Gaussian Model

We propose to consider a particularly simple Gaussian model with local interference only, as follows. Consider a set of nodes V, each $v \in V$ with a neighborhood N_v. The signal received by $v \in V$ is given by

$$Y_v \quad = \quad \tilde{Z}_v + \sum_{u \in N_v \setminus \{v\}} \frac{1}{d_{uv}^{\alpha/2}} X_u, \tag{60}$$

where $\tilde{Z}_v$ is i.i.d. Gaussian noise of zero mean and unit variance, α is the path loss exponent, and d_{uv} denotes the distance between nodes u and v. The transmitted signals X_u are assumed to be individually power-constrained with power P. In the remainder we will consider a line network in which all distances between neighbours are equal, and thus, we will set $d_{uv} = 1$, without loss of generality. For the $L+1$ node Gaussian line network (60) reduces to

$$Y_i = \begin{cases} \tilde{Z}_0 + X_1, & \text{if } i = 0 \\ \tilde{Z}_i + X_{i-1} + X_{i+1}, & \text{if } 0 < i < L \\ \tilde{Z}_L + X_{L-1}, & \text{if } i = L. \end{cases} \tag{61}$$

B. $\mathsf{P/P}$ Model

In this section we will outline how the Gaussian line network can be reduced to the $\mathsf{P/P}$ model. In the first step of the procedure we need to find suitable error correcting codes that turn the network into a reliable point-to-point link. Obviously, standard error correcting codes can be used. It remains to determine the maximum rate that can be achieved on each link. Since, under the $\mathsf{P/P}$ model, all interference is avoided, this maximum rate is simply the standard AWGN capacity. The second step of the procedure involves application of Theorem 1. Note that Theorem 1 is based on the assumption that the link capacity is one. Taking into account that in the reduced Gaussian model the link capacity is

$$\frac{1}{2} \log_q (1 + P) \tag{62}$$

q-ary symbols per time slot, it follows from Theorem 1 that the resulting transport capacity is

$$C^{\text{line}}_{\mathsf{P/P}}(L, P) = \left\lceil \frac{1}{2} L \right\rceil \frac{1}{2} \log_q (1 + P) \tag{63}$$

q-ary symbols$\times$hops per time slot.

C. $\mathsf{B/M}$ Model

The reduction of the Gaussian model to a $\mathsf{P/P}$ model involves only the use of standard error correcting codes. More interestingly, exploiting recent advances, we can also reduce the Gaussian network to the $\mathsf{B/M}$ model. In particular, consider the single multiple-access channel to node i, with $0 < i < L$, as in (61). Transmitters $i-1$ and $i+1$ both have a q-ary message. Now suppose that the receiver attempts to decode the sum of both q-ary messages.

This problem has been studied in [6], where it was shown that the maximum achievable rate R for which the sum can be reliably decoded satisfies

$$\frac{1}{2}\log_q\left(\frac{1}{2}+P\right) \leq R \leq \frac{1}{2}\log_q(1+P). \tag{64}$$

We note that this involves the use of lattice codes in a particular fashion, but we refer the reader to [6] for further details. Using this formula and Theorem 4, we can infer that

$$C^{\text{line}}_{\mathsf{B/M}}(L,P) \quad \geq \quad \frac{L}{2}\log_q\left(\frac{1}{2}+P\right). \tag{65}$$

q-ary symbols$\times$hops per time slot can be achieved.

Note, that

$$\lim_{L\to\infty}\lim_{P\to\infty}\frac{C^{\text{line}}_{\mathsf{B/M}}(L,P)}{C^{\text{line}}_{\mathsf{P/P}}(L,P)} \geq \lim_{L\to\infty}\frac{L}{\lceil\frac{1}{2}L\rceil} = 2. \tag{66}$$

Hence the multiplicative improvement obtained by moving from the $\mathsf{P/P}$ to the $\mathsf{B/M}$ model is the same in the Gaussian line network as in the deterministic network, for which this result was presented in Fig. 1. The results presented in this section provide a lower bound on the improvements in transport capacity that can be obtained by exploiting broadcast and interference in our Gaussian network, compared to reducing the network to point-to-point links. The reduction to the $\mathsf{B/M}$ deterministic model, using lattice codes, provides an achievable strategy that is not neccesarily optimal. The interesting point is that these lattice codes provide a means of exploiting interference that could be implemented in practice.

VIII. Discussion

Capacity bounds have been compared for four different deterministic models of wireless networks, representing four different ways of handling broadcast and superposition in the physical layer. These deterministic models have been inspired by recent studies on decoding functions of messages over a multiple access channel. One of the conclusion is that exploiting superposition and broadcast can lead to an increase in transport capacity of the hexagonal lattice of at least 150% and at most 500%.

We have presented a simple coding scheme for the hexagonal lattice under the $\mathsf{B/M}$ model. The proof techniques that have been introduced might be generalized to improve upper and lower bounds and to find more general coding schemes, both for the line and lattice networks and other network topologies. Of particular interest, would be to extend the results to random topologies.

We have made a connection between our deterministic models and Gaussian wireless networks. It will be of interest to extend these results to Gaussian models with more realistic interference models. Moreover, in order to apply these results in practice, decentralized coding and scheduling algorithms will need to be developed.

References

[1] R. Ahlswede, N. Cai, S.-Y. R. Li, and R. W. Yeung, “Network information flow,” *IEEE Trans. Inf. Theory*, vol. 46, no. 4, pp. 1204–1216, 2000.

[2] R. Yeung, *Information Theory and Network Coding*. Springer, 2008.

[3] C. Fragouli and E. Soljanin, "Network coding fundamentals," *Foundations and Trends® in Networking*, vol. 2, no. 1, pp. 1–133, 2007.

[4] ——, "Network coding applications," *Foundations and Trends® in Networking*, vol. 2, no. 2, pp. 135–269, 2007.

[5] B. Nazer and M. Gastpar, "Reliable computation over multiple-access channels," in *43rd Annual Allerton Conference*, Monticello, IL, September 2005.

[6] ——, "Computation over multiple-access channels," *IEEE Trans. Inf. Theory*, vol. 53, no. 10, pp. 3498–3516, 2007.

[7] Y. Wu, P. A. Chou, and S.-Y. Kung, "Information exchange in wireless networks with network coding and physical-layer broadcast," in *Proc. 39th Annual Conference on Information Sciences and Systems (CISS)*, 2005.

[8] S. Katti, H. Rahul, W. Hu, D. Katabi, M. Médard, and J. Crowcroft, "XORs in the air: practical wireless network coding," in *Proc. of ACM SIGCOMM*, 2006, pp. 243–254.

[9] C. Fragouli, J. Widmer, and J.-Y. Le Boudec, "Efficient broadcasting using network coding," *IEEE/ACM Trans. Netw.*, vol. 16, no. 2, pp. 450–463, 2008.

[10] A. Goel and S. Khanna, "On the network coding advantage for wireless multicast in euclidean space," in *Proceedings of the 7th international conference on Information processing in sensor networks*, 2008, pp. 64–69.

[11] J. Goseling, R. Matsumoto, T. Uyematsu, and J. Weber, "Lower bounds on the maximum energy benet of network coding for wireless multiple unicast," 2010, accepted for publication in Eurasip Journal on Wireless Communications and Networking, Special issue on network coding for wireless networks.

[12] J. K. Sundararajan, D. Shah, and M. Médard, "Feedback-based online network coding," 2009, arxiv, 0904.1730.

[13] P. Gupta and P. R. Kumar, "The capacity of wireless networks," *IEEE Trans. Inf. Theory*, vol. 46, no. 2, pp. 388–404, 2000.

[14] L. L. Xie and P. R. Kumar, "A network information theory for wireless communication: Scaling laws and optimal operation," *IEEE Trans. Inf. Theory*, vol. 50, no. 5, pp. 748–767, 2004.

[15] A. Ozgur, O. Leveque, and D. Tse, "Hierarchical cooperation achieves optimal capacity scaling in ad hoc networks," *IEEE Trans. Inf. Theory*, vol. 53, no. 10, pp. 3549 –3572, oct. 2007.

[16] R. Dougherty, C. Freiling, and K. Zeger, "Insufficiency of linear coding in network information flow," *IEEE Trans. Inf. Theory*, vol. 51, no. 8, pp. 2745–2759, 2005.

[17] A. Avestimehr, S. Diggavi, and D. Tse, "A deterministic approach to wireless relay networks," in *Proceedings of Allerton Conference on Communication, Control, and Computing*, 2007.

[18] ——, "Wireless network information flow," in *Proceedings of Allerton Conference on Communication, Control, and Computing*, 2007.

[19] S. Yazdi and S. Savari, "A Max-Flow/Min-Cut Algorithm for a Class of Wireless Networks," in *ACM-SIAM Symposium on Discrete Algorithms (SODA 2010), Austin, Texas*, 2010.

[20] M. Goemans, S. Iwata, and R. Zenklusen, "An Algorithmic Framework for Wireless Information Flow," in *Proceedings of Allerton Conference on Communication, Control, and Computing*, 2009.

[21] J. Ebrahimi and C. Fragouli, "Combinatorial Algorithms for Wireless Information Flow," *Arxiv preprint arXiv:0909.4808*, 2009.

[22] S. Katti and D. Katabi, "Embracing wireless interference: Analog network coding," in *Proc. of the 2007 Conference on Applications, Technologies, Architectures, and Protocols for computer communications*, 2007, pp. 397–408.

[23] M. Amin Rahimian, A. Ayremlou, and F. Marvasti, "A general analog network coding for wireless systems with fading and noisy channels," 2010, arxiv, 1009.3797.

[24] S. Zhang, S. Liew, and P. Lam, "Hot topic: physical-layer network coding," in *Proc. of the 12th Annual International Conference on Mobile Computing and Networking*, 2006, pp. 358–365.

[25] S. Zhang, S. Liew, and L. Lu, "Physical layer network coding schemes over finite and infinite fields," in *Proc. IEEE Globecom 2008*, 2008.

[26] Y. Hao, D. Goeckel, Z. Ding, D. Towsley, and K. Leung, "Achievable rates of physical layer network coding schemes on the exchange channel," in *Military Communications Conference,(MILCOM-07)*, 2007.

[27] K. Lu, S. Fu, Y. Qian, and H.-H. Chen, "On capacity of random wireless networks with physical-layer network coding," *IEEE J.Sel. A. Commun.*, vol. 27, no. 5, pp. 763–772, 2009.

[28] C.-H. Liu, F. Xue, and J. G. Andrews, "Network coding with two-way relaying: Achievable rate regions and diversity-multiplexing tradeoffs," 2009, arxiv, 0902.2260.

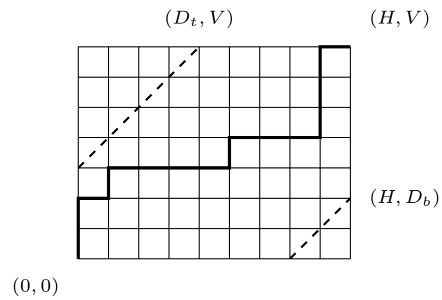

Fig. 19. A subset of the rectangular lattice, diagonals crossing (D_t, V) and (H, D_b) and a path from $(0, 0)$ to (H, V). In this figure: $H = 9$, $V = 7$, $D_t = 4$, $D_b = 2$.

[29] K. Narayanan, M. Wilson, and A. Sprintson, "Joint physical layer coding and network coding for bi-directional relaying," in *45th Annual Allerton Conference*, 2007.

[30] H. Saffar and P. Mitran, "Capacity bounds and lattice coding for the star relay network," 2010, arxiv, 1001.3708.

[31] S. Tang, O. Shagdar, H. Yomo, M. Shirazi, R. Suzuki, and S. Obana, "Layer-2 retransmission and combining for network coding-based forwarding in wireless networks," in *11th IEEE Singapore International Conference on Communication Systems, 2008. ICCS 2008*, 2008, pp. 1597–1602.

[32] W. Nam, S.-Y. Chung, and Y. H. Lee, "Nested lattice codes for gaussian relay networks with interference," 2009, arxiv, 0902.2436.

[33] B. Nazer and M. Gastpar, "Computing over multiple-access channels with connections to wireless network coding," in *Proceedings of the 2006 International Symposium on Information Theory (ISIT 2006)*, Seattle, WA, July 2006.

[34] B. Bollobás, *Modern graph theory*. Springer Verlag, 1998.

[35] R. M. Karp, "Reducibility among combinatorial problems," in *Complexity of Computer Computations*, R. E. Miller and J. W. Thatcher, Eds., 1972, pp. 85–103.

[36] K. Jain, J. Padhye, V. Padmanabhan, and L. Qiu, "Impact of interference on multi-hop wireless network performance," *Wireless networks*, vol. 11, no. 4, pp. 471–487, 2005.

[37] T. Cover and J. Thomas, *Elements of information theory*. Wiley, 1996.

[38] R. P. Stanley, *Enumerative combinatorics, Volume 2*. Cambridge University Press, 1999.

[39] E. Lucas, "Théorie des fonctions numériques simplement périodiques," *American Journal of Mathematics*, vol. 1, no. 2–4, pp. 184–240, 289–321, 1878.

Appendix A
Proof of Lemma 20

Part of the proof of Lemma 20 consists of a reduction to counting paths in a rectangular lattice. Therefore we start this appendix with a definition of this problem and a result concerning the number of such paths. Let D_t, D_b, $H > 0$ and $V > 0$ be integers. Consider the rectangular lattice and two of its diagonals; one diagonal through the points $\{(D_t + i, V + i)\}_{i \in \mathbb{Z}}$, the other through the points $\{(H + i, D_b + i)\}_{i \in \mathbb{Z}}$. The problem that we are concerned with is that of counting monotonic paths from $(0, 0)$ to (H, V) in the rectangular lattice that do not cross the diagonals. Monotonic paths are those paths that only move up or right in each step. In the remainder of this appendix, unless specificed otherwise, all paths under consideration are monotonic. A subset of the rectangular lattice, the diagonals, and a valid path are depicted in Fig. 19. The following lemma gives this number under the

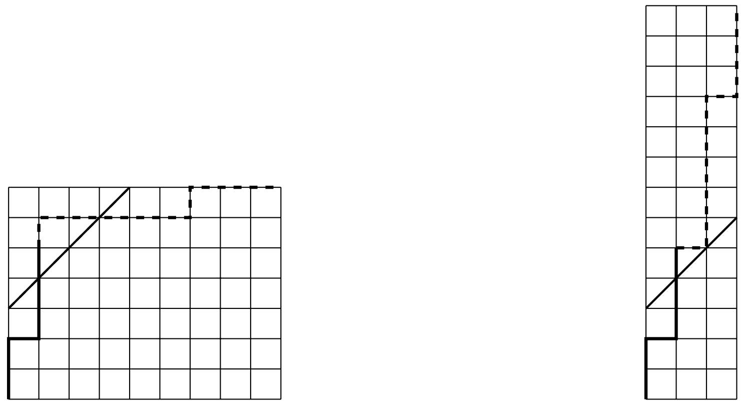

(a) Path crossing the diagonal.

(b) Path obtained after reflecting the part of the path after the first edge crossing the diagonal.

Fig. 20. Reflection principle. There is a one-to-one correspondence between the set of diagonal-crossing paths in Fig. 20(a) and the set of paths in Fig. 20(b).

assumption that no monotonic path can cross both diagonals. We follow the convention that $\binom{n}{k} = 0$, if $k < 0$.

Lemma 22. *Let D_t, D_b, $H > 0$ and $V > 0$ be integers. Consider the two-dimensional rectangular grid and two of its diagonals crossing (D_t, V) and (H, D_b). Assume $D_t \leq H - D_b$ and $D_b \leq V - D_t$. Then the number of monotic paths in the grid from $(0, 0)$ to (H, V) that do not cross the diagonals is*

$$\binom{H+V}{H} - \binom{H+V}{D_t - 1} - \binom{H+V}{D_b - 1}. \tag{67}$$

Proof: Note that all paths are of length $H + V$. Moreover, any path needs H steps to the right and V steps up. Therefore, the total number paths equals $\binom{H+V}{H}$. The two other terms in (67) correspond to the number of paths crossing the top and bottom diagonal respectively. The assumption that $D_t \leq H - D_b$ and $D_b < V - D_t$ ensures that there are no paths that cross both diagonals. The number of paths crossing the top diagonal can be found using a reflection principle, a technique that is widely used in the area of combinatorics, *cf.* [38]. There is a one-to-one correspondence between the set of paths from $(0, 0)$ to (H, V) that cross the top diagonal and the total number of paths from $(0, 0)$ to $(D_t - 1, H + V - D_t + 1)$. The mapping giving the correspondence consists of reflecting (replacing a move right, by a move up, and vice versa) the part of the path after the first edge crossing the diagonal. This reflection principle is illustrated in Fig. 20. Now it directly follows that the number of paths that cross the top diagonal is $\binom{H+V}{D_t-1}$. In the same way it follows that the number of paths crossing the bottom diagonal is $\binom{H+V}{D_b-1}$. ■

Note, that the problem of counting paths in the rectangular lattice with two diagonals is very similar to counting Dyck paths, *cf.* [38]. The differences with counting Dyck paths are that instead of one diagonal we have two

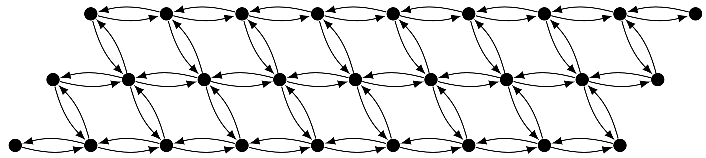

Fig. 21. Graph (V, E').

diagonals. Dyck paths, moreover, would start and end at the diagonal. Various generalizations have been considered in literature [38], but we are not aware of results related to our counting problem.

Next we present a standard result on congruence relations for binomial coefficients.

Theorem 9 (Lucas [39])**.** *Let c be a prime number and let a and b, $a \geq b$, be positive integers written in base c, i.e., let $a = \sum_{i=0}^{s} a_i c^i$ and $b = \sum_{i=0}^{t} b_i c^i$ with $0 \leq a_i < c$, $0 \leq b_i < c$, $a_s \neq 0$, $b_t \neq 0$ and $s \geq t$. Then*

$$\binom{a}{b} \equiv \prod_{i=0}^{t} \binom{a_i}{b_i} \pmod{c}. \tag{68}$$

We will be using the following corollary to Lucas' Theorem.

Corollary 1. *Let κ and b be positive integers, $b < 2^\kappa$. Then $\binom{2^\kappa}{b} \equiv 0 \pmod{2}$.*

Proof: Since $0 < b < 2^\kappa$, we have $b = \sum_{i=0}^{t} b_i 2^i$, where $0 < t < \kappa$ and $b_t = 1$. From Theorem 9 we have

$$\binom{2^\kappa}{b} \equiv \prod_{i=0}^{t} \binom{0}{b_i} \pmod{2} \equiv 0 \pmod{2}. \tag{69}$$

■

We make the following observation on even-odd scheduling together with simple retransmissions. Suppose that a node (u_1, u_2) is transmitting. Then, the following nodes are receiving from (u_1, u_2):

$$(u_1 - 1, u_2 + 1), \quad (u_1 - 1, u_2), \quad (u_1 + 1, u_2), \quad (u_1 + 1, u_2 - 1).$$

Therefore, we associate with a hexagonal network (V, E) that is operated in this fashion, a graph (V, E'), where

$$E' = \left\{ ((u_1, u_2), (v_1, v_2)) \in V \times V \,\middle|\, (v_1, v_2) \in \left\{ (u_1{+}1, u_2), (u_1{+}1, u_2{-}1), (u_1{-}1, u_2), (u_1{-}1, u_2{+}1) \right\} \right\}. \tag{70}$$

The graph (V, E') is depicted in Fig. 21 for $L = 8$ and $M = 2$. One can easily verify the following lemma, which is therefore given without a proof.

Lemma 23. *Assume even-odd scheduling and simple retransmissions over $\mathbb{F}_2$ on a hexagonal network (V, E). Suppose that in time slot $t = 0$ node (u_1, u_2) transmits a symbol m and all other nodes transmit 0. Then at time t node (v_1, v_2) transmits symbol m iff in the graph (V, E') the number of paths from (u_1, u_2) to (v_1, v_2) of length t is odd. Nodes not transmitting the symbol m are transmitting zero.*

Note that these paths need not be simple, *i.e.*, they can use the same vertices and edges multiple times. This implies that paths can contain cycles. In order to simplify the discussion we introduce some notation. There are four types of edges in the graph (V, E'), these types will be denoted as

$$\mathsf{l}: \quad \text{for edges of type } \Big((u_1, u_2), (u_1 - 1, u_2)\Big), \tag{71}$$

$$\mathsf{r}: \quad \text{for edges of type } \Big((u_1, u_2), (u_1 + 1, u_2)\Big), \tag{72}$$

$$\mathsf{u}: \quad \text{for edges of type } \Big((u_1, u_2), (u_1 - 1, u_2 + 1)\Big), \tag{73}$$

$$\mathsf{d}: \quad \text{for edges of type } \Big((u_1, u_2), (u_1 + 1, u_2 - 1)\Big), \tag{74}$$

where the l(eft), r(ight), u(p) and d(own) denote the movement made from the perspective of (u_1, u_2). Note that movements u and d are also affecting the value of the first coordinate. Hence, naming these up-left and down-right would have been more accurate. Given the starting vertex of a path, it can be represented in terms of a sequence from $\{\mathsf{l}, \mathsf{r}, \mathsf{u}, \mathsf{d}\}^*$, representing the moves taken from the starting vertex. The superscript * is used to denote the union of the k-ary Cartesian products, $k \in \mathbb{N}$. Since we will consider sets of paths starting from the same vertex, we will represent paths only by the sequence of moves. Let $P(s)$ be the subsequence, restricted to u and d movements, of a sequence $s \in \{\mathsf{l}, \mathsf{r}, \mathsf{u}, \mathsf{d}\}^*$. For $s = \mathsf{l\,u\,l\,u\,d\,r\,l\,u\,d}$, for instance, we have $P(s) = \mathsf{u\,u\,d\,u\,d}$. Finally, let $\mathsf{l}(s)$, $\mathsf{r}(s)$, $\mathsf{u}(s)$ and $\mathsf{d}(s)$ be the number of occurences of respectively l, r, u and d in s.

The proof of Lemma 20, the aim of this appendix, is a direct consequence of Lemma 23 and the following Lemma 24.

Lemma 24. *Given (V, E') of size $(L+1) \times (M+1)$, where $M = 2^\kappa - 2$, $\kappa \geq 2$ and $L \geq 2^{\kappa+1}$. Let $(u_1, u_2) \in V$, $(v_1, v_2) \in V$, where $2^\kappa \leq u_1 \leq L - 2^\kappa$. Let A be the number of paths of length 2^κ from (u_1, u_2) to (v_1, v_2). We have*

$$A \equiv \begin{cases} 1 \pmod 2, & \text{if } |v_1 - u_1| = 2^\kappa \text{ and } v_2 = u_2, \\ 0 \pmod 2, & \text{otherwise}. \end{cases} \tag{75}$$

Proof: Let $n = 2^\kappa$. W.l.o.g. consider $v_1 - u_1 \geq 0$. Moreover, we consider $v_1 - u_1$ even, since, if $v_1 - u_1$ is odd there are no paths of length n from (u_1, u_2) to (v_1, v_2). Let $\mathcal{A}$ be the set of all paths of length n from (u_1, u_2) to (v_1, v_2). We partition $\mathcal{A}$ into sets of paths that have the same $\{\mathsf{u}, \mathsf{d}\}^*$ subsequence, *i.e.*, for $p \in \{\mathsf{u}, \mathsf{d}\}^*$ let

$$\mathcal{A}_p = \big\{ s \in \mathcal{A} \big| P(s) = p \big\}. \tag{76}$$

Note that there are many p for which $\mathcal{A}_p$ is empty, since not all p can lead to a valid path from (u_1, u_2) to (v_1, v_2). The sequence $\mathsf{u\,u} \cdots \mathsf{u\,u}$ of length n, for instance, is not a valid path in (V, E), since it would ‘cross the boundary’ of the graph. Also, there are p that can not lead to a path that ends in (v_1, v_2). More precisely, we have the following basic constraints. First, we need

$$\mathsf{u}(s) - \mathsf{d}(s) = u_2 - v_2. \tag{77}$$

Moreover, we need $(\mathsf{r}(s)+\mathsf{d}(s))-(\mathsf{l}(s)+\mathsf{u}(s))=v_1-u_1$. Combined with $\mathsf{l}(s)+\mathsf{r}(s)+\mathsf{u}(s)+\mathsf{d}(s)=n$ this leads to

$$\mathsf{l}(s)+\mathsf{u}(s)=\frac{n-v_1+u_1}{2}, \tag{78}$$

$$\mathsf{r}(s)+\mathsf{d}(s)=\frac{n+v_1-u_1}{2}. \tag{79}$$

Since we consider v_1-u_1 even, $(n-v_1+u_1)/2$ and $(n+v_1-u_1)/2$ are integers.

Let $A_p=|\mathcal{A}_p|$. Now,

$$A=\sum_{k=0}^{n}\sum_{p\in\{\mathsf{u},\mathsf{d}\}^k}A_p=A_\emptyset+\sum_{k=1}^{n-1}\sum_{p\in\{\mathsf{u},\mathsf{d}\}^k}A_p+\sum_{p\in\{\mathsf{u},\mathsf{d}\}^n}A_p. \tag{80}$$

The following claims, which will be proved in the remainder, prove the lemma:

1) $A_\emptyset\equiv\begin{cases}1 \pmod 2, & \text{if } |v_1-u_1|=2^\kappa \text{ and } v_2=u_2,\\ 0 \pmod 2, & \text{otherwise,}\end{cases}$
2) $A_p\equiv 0 \pmod 2$ for $1\le|p|\le n-1$,
3) $\sum_{p\in\{\mathsf{u},\mathsf{d}\}^n}A_p\equiv 0 \pmod 2$.

For Claim 1 note that if $u_2\neq v_2$ we have $A_\emptyset=0$ because constraint (77) is not satisfied. For $u_2=v_2$ we need to show that $A_\emptyset\equiv 1 \pmod 2$ iff $v_1-u_1=n$. Note that $A_\emptyset=\binom{n}{\mathsf{l}(s)}$. From $\mathsf{u}(s)=0$ and (78) it follows that $\mathsf{l}(s)=(n-v_1+u_1)/2$. Hence, if $v_1-u_1<n$ then $0<\mathsf{l}(s)<n$, and Corollary 1 gives $\binom{n}{\mathsf{l}(s)}\equiv 0 \pmod 2$. If $v_1-u_1=n$, then $\mathsf{l}(s)=0$ and $\binom{n}{\mathsf{l}(s)}=1$.

For Claim 2 we show that $A_p\equiv 0 \pmod 2$ by giving an explicit construction of the sequences in $\mathcal{A}_p$. The construction is in two phases. We start from a length n sequence with undefined entries. In the first phase, the sequence p is embedded in this length n sequence. In the second phase the remaining undefined entries are filled with l and r moves. There are $\binom{n}{|p|}$ ways to perform the first phase. By Corollary 1, since $1\le|p|\le n-1$, we have $\binom{n}{|p|}\equiv 0 \pmod 2$. The number of ways to perform the second phase is independent of the result of the first phase. A_p is, therefore, a multiple of $\binom{n}{|p|}$, proving Claim 2.

For the proof of Claim 3 first note that

$$\sum_{p\in\{\mathsf{u},\mathsf{d}\}^n}A_p=\left|\left\{s\in\mathcal{A}\,\middle|\,\mathsf{l}(s)=\mathsf{r}(s)=0\right\}\right|, \tag{81}$$

i.e., we are counting the paths of length n from (u_1,u_2) to (v_1,v_2) that have only u and d moves. The constraints (77)–(79) reduce to

$$\mathsf{u}(s)=\frac{n-v_1+u_1}{2}, \tag{82}$$

$$\mathsf{d}(s)=\frac{n+v_1-u_1}{2}. \tag{83}$$

The problem of counting the paths that satisfy these constraints is tackled by reducing it to counting monotonic paths in the rectangular lattice, for which a result was presented in Lemma 22. In the rectangular lattice consider monotonic paths from $(0,0)$ to $((n-v_1+u_1)/2,(n+v_1-u_1)/2)$. Note that length of these paths is always n.

By associating a u move in (V, E') to a move up in the rectangular lattice and a d move in (V, E') with a right move in the rectangular lattice, we see that there is a one-to-one correspondence between paths of u and d moves in (V, E') and monotonic paths from $(0, 0)$ to $(n - v_1 + u_1)/2 \times (n + v_1 - u_1)/2$ in the rectangular lattice.

In addition to the constraints on $\mathsf{u}(s)$ and $\mathsf{d}(s)$, the top and bottom borders of (V, E') impose constraints on the sequences corresponding to valid paths. Starting with the constraint imposed by the top border, note that a path starting from (u_1, u_2) can start with at most $n - 2 - u_2$ consecutive u moves. Also, after each d move, an additional u move is allowed. Therefore, the constraint imposed by the top border of (V, E') corresponds to a diagonal crossing $(0, n - 2 - u_2)$ in the rectangular lattice. A path in the lattice corresponding to a valid path in (V, E') can not cross this diagonal. In similar fashion it follows that the bottom border of (V, E') imposes a constraint in the form of a diagonal crossing $(u_2, 0)$ in the rectangular lattice. Note that the diagonal crossing in $(u_2, 0)$ also crosses in $((n+v_1-u_1)/2, (n+v_1-u_1)/2-u_2)$. The diagonal crossing in $(0, n-2-u_2)$ also crosses in $((n - v_1 + u_1)/2, (n - v_1 + u_1)/2 - (n - 2 - u_2))$. In terms of Lemma 22 we have reduced our problem to counting monotonic paths from $(0, 0)$ to $((n - v_1 + u_1)/2, (n + v_1 - u_1)/2)$ in the rectangular lattice, not crossing the diagonals $((n - v_1 + u_1)/2, (n - v_1 + u_1)/2 - (n - 2 - u_2))$ and $((n + v_1 - u_1)/2, (n + v_1 - u_1)/2 - u_2)$. From Lemma 22 we obtain

$$\sum_{p \in \{\mathsf{u},\mathsf{d}\}^n} A_p = \binom{n}{\frac{n-v_1+u_1}{2}} - \binom{n}{\frac{n-v_1+u_1}{2} - (n-2-u_2) - 1} - \binom{n}{\frac{n+v_1-u_1}{2} - u_2 - 1}. \tag{84}$$

Observe that the first term is always even. The second term is odd iff

$$(n - v_1 + u_1)/2 - (n - 2 - u_2) - 1 = 0 \quad \Longrightarrow \quad u_2 = \frac{n + v_1 - u_1}{2} - 1. \tag{85}$$

The third term is odd iff

$$(n + v_1 - u_1)/2 - u_2 - 1 = 0 \quad \Longrightarrow \quad u_2 = \frac{n + v_1 - u_1}{2} - 1. \tag{86}$$

From (85) and (86) it follows that the sum of the second and third term in (84) is always even. ■